













# NAVAL POSTGRADUATE SCHOOL

## Monterey, California



### THESIS

B36446

ATMOSPHERIC ANGULAR MOMENTUM AND  
LENGTH OF DAY

by

William L. Benedict

March 1988

Thesis Advisor

Robert L. Haney

Approved for public release; distribution is unlimited.

T238697





Unclassified

Security classification of this page

## REPORT DOCUMENTATION PAGE

1a Report Security Classification <b>Unclassified</b>			1b Restrictive Markings		
2a Security Classification Authority			3 Distribution Availability of Report		
4b Declassification Downgrading Schedule			Approved for public release; distribution is unlimited.		
5 Performing Organization Report Number(s)			5 Monitoring Organization Report Number(s)		
6a Name of Performing Organization Naval Postgraduate School		6b Office Symbol (if applicable) 35	7a Name of Monitoring Organization Naval Postgraduate School		
6c Address (city, state, and ZIP code) Monterey, CA 93943-5000			7b Address (city, state, and ZIP code) Monterey, CA 93943-5000		
8a Name of Funding Sponsoring Organization		8b Office Symbol (if applicable)	9 Procurement Instrument Identification Number		
8c Address (city, state, and ZIP code)			10 Source of Funding Numbers		
			Program Element No	Project No	Task No
			Work Unit Accession No		
11 Title (include security classification) <b>ATMOSPHERIC ANGULAR MOMENTUM AND LENGTH OF DAY</b>					
12 Personal Author(s) <b>William L. Benedict</b>					
13a Type of Report Master's Thesis		13b Time Covered From To		14 Date of Report (year, month, day) March 1988	15 Page Count 63
16 Supplementary Notation The views expressed in this thesis are those of the author and do not reflect the official policy or position of the Department of Defense or the U.S. Government.					
17 Cosati Codes			18 Subject Terms (continue on reverse if necessary and identify by block number)		
Field	Group	Subgroup	Length of Day, Atmospheric Angular Momentum		
19 Abstract (continue on reverse if necessary and identify by block number)					
<p>Changes in the globally integrated absolute angular momentum of the atmosphere were computed from the Fleet Numerical Oceanography Center NOGAPS wind analyses and compared to astronomically measured changes in length of day (LOD) obtained from the U.S. Naval Observatory, Washington D.C. The two time series were subjected to both time and frequency domain analysis. In the time domain, digital filters were used to isolate seasonal and subseasonal components. In the frequency domain, energy density, coherence and phase were computed over periods from 2 days to 1000 days. Over 90% of the total variance in astronomically determined LOD can be explained by meteorological phenomena. Fluctuations in LOD are coherent and in phase with fluctuations in the globally integrated angular momentum of the Earth's shell (crust, mantle and oceans; liquid core is excluded) at almost all periods less than 365 days. Annual fluctuations in LOD appear to originate in the midlatitudes and propagate equatorward. Subseasonal fluctuations (30 to 100 day periods) appear to be a tropical phenomena.</p>					
20 Distribution Availability of Abstract <input checked="" type="checkbox"/> unclassified unlimited <input type="checkbox"/> same as report <input type="checkbox"/> DTIC users			21 Abstract Security Classification Unclassified		
22a Name of Responsible Individual Robert L. Haney			22b Telephone (include Area code) (408) 646-2044	22c Office Symbol 63Hy	

DD FORM 1473,84 MAR

83 APR edition may be used until exhausted  
All other editions are obsolete

Security classification of this page

Unclassified

Approved for public release; distribution is unlimited.

Atmospheric Angular Momentum and Length of Day

by

William L. Benedict  
Commander, United States Navy  
B.A., University of Michigan, 1971

Submitted in partial fulfillment of the  
requirements for the degree of

MASTER OF SCIENCE OCEANOGRAPHY AND METEOROLOGY

from the

NAVAL POSTGRADUATE SCHOOL  
March 1988

---

## ABSTRACT

Changes in the globally integrated absolute angular momentum of the atmosphere were computed from the Fleet Numerical Oceanography Center NOGAPS wind analyses and compared to astronomically measured changes in length of day (*LOD*) obtained from the U.S. Naval Observatory, Washington D.C. The two time series were subjected to both time and frequency domain analysis. In the time domain, digital filters were used to isolate seasonal and subseasonal components. In the frequency domain, energy density, coherence and phase were computed over periods from 2 days to 1000 days. Over 90% of the total variance in astronomically determined *LOD* can be explained by meteorological phenomena. Fluctuations in *LOD* are coherent and in phase with fluctuations in the globally integrated angular momentum of the Earth's shell (crust, mantle and oceans; liquid core is excluded) at almost all periods less than 365 days. Annual fluctuations in *LOD* appear to originate in the midlatitudes and propagate equatorward. Subseasonal fluctuations (30 to 100 day periods) appear to be a tropical phenomena.

## TABLE OF CONTENTS

I. INTRODUCTION AND THEORY .....	1
A. BACKGROUND .....	1
B. ASTRONOMIC LENGTH OF DAY .....	2
C. ATMOSPHERIC ANGULAR MOMENTUM AND LENGTH OF DAY ..	4
II. DATA ACQUISITION AND PROCESSING .....	8
A. U.S. NAVAL OBSERVATORY LOD MEASUREMENTS .....	8
B. NOGAPS WIND DATA .....	8
C. ANALYSIS TECHNIQUES .....	9
1. Time Domain Analysis .....	9
2. Frequency Domain Analysis .....	11
3. Harmonic Analysis .....	13
III. RESULTS .....	14
A. GLOBAL COMPARISON IN THE TIME DOMAIN .....	14
1. Seasonal Components .....	14
2. Subseasonal Components .....	15
B. GLOBAL COMPARISONS IN THE FREQUENCY DOMAIN .....	16
1. The Energy Density Spectra of $\delta LOD_{atm}$ and $\delta LOD_{USNO}$ .....	16
2. Coherence Spectrum .....	16
3. Phase Spectrum .....	17
4. Harmonic Analysis .....	17
C. LATITUDE COMPARISONS OF LOD .....	17
IV. SUMMARY .....	19
APPENDIX A. FORTRAN CODE FOR DECODING NEDN TAPES AND COMPUTING LOD .....	33
APPENDIX B. FORTRAN CODE FOR SPECTRAL ANALYSIS .....	41

APPENDIX C. FREQUENCY RESPONSE OF DIGITAL FILTERS .....	47
LIST OF REFERENCES .....	50
INITIAL DISTRIBUTION LIST .....	52

## LIST OF TABLES

Table 1.	LINEAR CORRELATION COEFFICIENTS .....	20
Table 2.	VARIANCES .....	21
Table 3.	PHASE AND AMPLITUDES OF LOD .....	21



## LIST OF FIGURES

Fig. 1. Unfiltered time series of $\delta LOD_{USNO}$ (top) and $\delta LOD_{atm}$ (bottom)	22
Fig. 2. Detrended $\delta LOD_{atm}$ and $\delta LOD_{USNO}$ series	22
Fig. 3. Smoothed $\delta LOD_{atm}$ and $\delta LOD_{USNO}$ series	23
Fig. 4. Seasonal terms of $\delta LOD_{atm}$ and $\delta LOD_{USNO}$	23
Fig. 5. Annual terms of $\delta LOD_{USNO}$ and $\delta LOD_{atm}$	24
Fig. 6. Semiannual terms of $\delta LOD_{USNO}$ and $\delta LOD_{atm}$	24
Fig. 7. Subseasonal Oscillations of $\delta LOD_{atm}$ and $\delta LOD_{USNO}$	25
Fig. 8. Comparison of $\delta LOD_{USNO-subseas}$ and $\delta LOD_{atm15}$	25
Fig. 9. Comparison of $\delta LOD_{USNO-seasonal}$ and $\delta LOD_{atm75}$	26
Fig. 10. Comparison of $\delta LOD_{USNO-subseas}$ and $\delta LOD_{atm20}$	26
Fig. 11. Comparison of $\delta LOD_{USNO-seasonal}$ and $\delta LOD_{atm70}$	27
Fig. 12. Energy Density, Coherence, and Phase Spectra of $\delta LOD_{atm}$ and $\delta LOD_{USNO}$	28
Fig. 13. Energy Density, Coherence, and Phase Spectra of $\delta LOD_{USNO}$ and $\delta LOD_{atm15}$	29
Fig. 14. Energy Density, Coherence, and Phase Spectra of $\delta LOD_{USNO}$ and $\delta LOD_{atm75}$	30
Fig. 15. Energy Density, Coherence, and Phase Spectra of $\delta LOD_{USNO}$ and $\delta LOD_{atm20}$	31
Fig. 16. Energy Density, Coherence, and Phase Spectra of $\delta LOD_{USNO}$ and $\delta LOD_{atm70}$	32
Fig. 17. Spectral response of 23-point $\sin^2$ weighted filter	47
Fig. 18. Spectral response of a twice run 75-point $\sin^2$ filter	47
Fig. 19. Response of 183-point unweighted moving average filter	48
Fig. 20. Filter to isolate semiannual terms	48
Fig. 21. Subseasonal isolation filter	49

## ACKNOWLEDGEMENTS

I am particularly grateful to Professor Robert Haney for his support and encouragement while researching and writing this paper. He patiently used his immense scientific and geophysical talents to teach me the fundamentals required to undertake this project. Professor Will Shaw provided me with time-consuming, personal instruction in statistical procedures and time series analysis methods.

I am grateful to Dr. Roland Madden of NCAR for his time and help in researching the causes of some of our results. Dr Jean Dickey of JPL also provided me with valuable background information as well as NMC weather data.

Finally, I am most grateful to my wife, Kathy, for her moral support and encouragement throughout my two years at Naval Postgraduate School.



# I. INTRODUCTION AND THEORY

## A. BACKGROUND

Fluctuations in the Earth's length of day (*LOD*) were surmised by early astronomers who noted cumulative irregularities in the Earth's expected latitudinal position relative to daily star transits. Newtonian physics explained only the tidal component of these short period changes in the Earth's angular momentum. In the late 1930's, pendulum clocks were accurate enough to measure daily star transits to within 1 ms.<sup>1</sup> Stoyko (1937, cited in Munk and MacDonald, 1960) reported a 2 ms cumulative seasonal variation in *LOD*. He noted that the length of day measured in July was longer than that measured in May by 2 ms. Atomic clocks, developed in the 1950's, improved time keeping accuracy by several orders of magnitude. Present day cesium clocks have accuracies better than  $10^{-8}$  s per day (or .00001 ms) (Ramsey, 1988). At the same time, improvements in astronomical measurement methods led to more precise determination of star and quasar transits.

A number of studies have been undertaken to link the observed changes in *LOD* to meteorological phenomena. Starr (1948, cited in Munk and MacDonald, 1960) proposed that the observed changes in the Earth's *LOD* occurred because the solid Earth and atmosphere exchanged angular momentum on a seasonal basis. Madden and Julian (1971) found 40-50 day oscillations in pressure and zonal winds centered in the tropics, and Lambeck and Cazenave (1974) subsequently linked these atmospheric oscillations to changes in *LOD*. Lambeck (1980) identified the amplitudes and phases of the seasonal changes and listed other, non meteorological components which could be responsible for *LOD* changes. Rosen and Salstein (1983) correlated short period (less than seasonal) hemispherical changes of atmospheric angular momentum and *LOD* with polar and subtropical jet streams. Eubanks *et al.* (1985) performed a spectral analysis of atmospherically derived angular momentum with a composite of astronomic, satellite and Lunar Laser Ranging (LLR)<sup>2</sup> *LOD* data. Barnes *et al.* (1983) extensively studied

---

<sup>1</sup> The best gravity pendulum clocks have accuracies within 1 ms per day or one part in  $10^8$  (Ramsey, 1988). This is barely accurate enough to detect the fairly large seasonal changes in the *LOD*.

<sup>2</sup> The astronauts left a corner reflector on the moon which reflects a LASER signal back for extremely accurate short term measurement of Earth rotation parameters.

changes in *LOD* over the period 1979-1981. Morgan *et al.* (1985) used least squares analysis to study the seasonal as well as subseasonal nature of oscillations in the *LOD* from 1981 to 1984. Swinbank (1985) examined the torques which produce changes in *LOD*. Wolf and Smith (1987), and Eubanks *et al.* (1986) compared changes in atmospheric angular momentum with astronomically determined *LOD* during the El Nino of 1983.

Most studies have examined atmospheric angular momentum and *LOD* using time measurements from the Bureau International de l'Heure (BIH), augmented by LLR and other precise rotation measurement methods, to compare with gridded zonal wind data from the U.S. National Meteorological Center (NMC) or the European Centre for Medium Range Weather Forecasts (ECMWF). This paper analyzes the wind-derived atmospheric angular momentum budget for the period January 1983 to July 1987 and the simultaneous changes in the Earth's *LOD* using time data from the U.S. Naval Observatory (USNO) and zonal wind data from the U.S. Navy Fleet Numerical Oceanography Center NOGAPS model.<sup>3</sup> The atmospheric angular momentum changes are then examined over two latitude bands to investigate the horizontal structure of the seasonal and subseasonal components of the atmospheric angular momentum and contributions to the *LOD*.

## B. ASTRONOMIC LENGTH OF DAY

Astronomic length of day is measured by comparing elapsed time for meridional transits of stars or quasars with a reference time determined by atomic clocks. The time it takes for exactly one rotation of the Earth (360 degrees of longitude change) with respect to the fixed, inertial reference system of distant stars is a sidereal day with a mean value of 86,164.0905 seconds. Earth time is generally kept with respect to rotation about the sun: the solar day. A mean solar day is slightly longer and subject to more variability than the sidereal day because the Earth is in motion about the sun. Time for a solar day (*LOD<sub>s</sub>*) is defined as exactly 86,400 seconds. *LOD* is defined as the actual elapsed time (measured by cesium clocks) for a meridional transit of a point on Earth with respect to an inertial frame. Since this is with respect to sidereal time, a conversion is applied to make it consistent with solar time keeping.

---

<sup>3</sup> NOGAPS is Naval Operational Global Atmospheric Prediction System. It is a mathematical model which generates a global wind and pressure analysis on a 2 ½ by 2 ½ degree grid spacing.

$LOD$  is related to the Earth rotation rate ( $\omega$ ) by:

$$\omega = \Omega \frac{LOD_o}{LOD} = \Omega \frac{d(UT1)}{d(IAT)}, \quad (1)$$

where  $LOD$  and  $UT1$  are both measures of the actual elapsed time of the solar day,  $\Omega$  is the mean sidereal rotation rate ( $7.2921 \times 10^{-5} \text{ s}^{-1}$ ) of the Earth, and  $IAT$  is the precise time reference determined from atomic clocks.  $UT1$  is an angular measurement of Earth's polar rotation with respect to sidereal time passage which is usually converted to time.

Changes in the Earth's rotation rate with respect to accepted standard values are:<sup>4</sup>

$$\delta\omega \equiv \Omega \frac{LOD_o}{LOD} - \Omega \frac{LOD_o}{LOD_{std}} = \Omega \frac{d(UT1 - IAT_{std})}{dt}. \quad (2)$$

Taking the difference between  $LOD$  and the standard,  $LOD_{std}$ , to be  $\delta LOD$  produces:

$$\delta\omega = -\Omega \frac{\delta LOD}{LOD} \simeq -\Omega \frac{\delta LOD}{LOD_o} = \Omega \frac{d(UT1 - IAT_{std})}{dt}, \quad (3)$$

where  $LOD_{std}$  is taken equal to  $LOD_o$  and  $IAT_{std}$  is taken equal to a sidereal day, although other conventions could be used with the relationship still holding (Eubanks *et al.*, 1985). The approximation in (3) is valid because, using a time step of one sidereal day,  $LOD_o$ , the ratio of  $\delta LOD$  to  $LOD$  is the same as the ratio of  $\delta LOD$  to  $LOD_o$  to within  $10^{-8}$ s. Using finite differences to approximate the  $UT1$  derivative:

$$\delta LOD = -LOD_o \left( \frac{(UT1 - IAT_{std})_t - (UT1 - IAT_{std})_{t-\Delta t}}{\Delta t} \right). \quad (4)$$

Eq. 4 relates daily observations of star and quasar transits directly with the precise elapsed time determined by atomic clocks. It is computed on a daily basis ( $\Delta t = 1$  day) from astronomic data gathered all over the world to help eliminate single site bias. This

---

<sup>4</sup> By subtracting standard values, which are the international definitions of the solar and sidereal days, the remaining quantity represents a change from the standard as well as a change with respect to exactly one solar day. The actual measured length of day is taken with reference to a beginning epoch (1 January 1900, by convention). Thus the actual length of day ( $LOD$ ) is the running sum of the changes in  $LOD$  from the beginning of the epoch. Thus, the term  $\delta LOD$ , as developed in Eq. 4 represents a time derivative only in the sense of it being the first difference of the  $LOD$  time series. If the first difference were not used, the numbers associated with the length of day would be so large as to be cumbersome.



quantity is compared with the atmospherically derived equivalent,  $\delta LOD_{\text{atm}}$ , developed in the next section.

### C. ATMOSPHERIC ANGULAR MOMENTUM AND LENGTH OF DAY

Over long periods of time (centuries and longer) Earth angular momentum ( $M_{\text{Earth}}$ ) slowly transfers to the moon through solid body tidal friction; hence  $LOD$  increases slowly and  $M_{\text{Earth}}$  decreases. For periods less than 10 years, this effect is negligible;  $M_{\text{Earth}}$  is essentially conserved (Eubanks *et al.*; 1985, Lambeck, 1980). Thus, changes in  $M_{\text{Earth}}$ , denoted by  $\delta M_{\text{Earth}}$  will sum to zero:

$$\delta M_{\text{Earth}} = \delta M_{\text{shell}} + \delta M_{\text{ocean}} + \delta M_{\text{atm}} + \delta M_{\text{core}} = 0. \quad (5)$$

Since  $\delta M_{\text{core}}$  and  $\delta M_{\text{shell}}$  interact in an oscillatory manner with a period of 10 years or greater,  $\delta M_{\text{core}}$  appears in short data records (under five years) as a linear trend and is easily removed by detrending. The three remaining momentum elements:  $\delta M_{\text{atm}}$ ,  $\delta M_{\text{shell}}$  and  $\delta M_{\text{ocean}}$  interact to produce changes in the Earth measured  $LOD$ .  $\delta M_{\text{ocean}}$  is difficult to measure directly. To exchange momentum with the rotating Earth, the oceans must have unimpeded zonal flow about the globe. Only the Antarctic Circumpolar Current (ACC) has such characteristics. Lambeck (1980) agrees with the earlier findings of Munk and MacDonald (1960) that, at most, the ACC could have a semiannual amplitude 5% of the atmospheric amplitudes. Thus, with  $\delta M_{\text{Earth}} = 0$ , and disregarding inputs from the ocean and core:

$$\delta M_{\text{shell}} = -\delta M_{\text{atm}}. \quad (6)$$

The atmosphere of the Earth represents about  $10^{-6}$  of the total mass of the solid Earth (solid Earth includes crust, mantle, oceans and atmosphere; everything except the liquid core). Because of the large difference in atmospheric and Earth masses, relatively large changes in the zonal velocity field of the atmosphere are required to produce small changes in  $M_{\text{shell}}$ .

The angular velocity ( $\omega$ ) of the Earth's shell (solid Earth minus the atmosphere) is:

$$\omega = \frac{M_{\text{shell}}}{I_{\text{shell}}}, \quad (7)$$

where  $M_{\text{shell}}$  is the angular momentum of the Earth's shell and  $I_{\text{shell}}$  is the polar moment of inertia. Again, after subtracting standard values from  $\delta M_{\text{shell}}$ , changes in  $\omega$  are:

$$\delta\omega = \frac{\delta M_{\text{shell}}}{\bar{I}_{\text{shell}}}. \quad (8)$$

Overbars indicate average values with respect to time. Since  $\bar{I}_{\text{shell}}$  changes little on time scales less than decades, it is taken as a constant:  $7.103 \times 10^{37} \text{ kg m}^2$ . Substituting  $-\delta M_{\text{atm}}$  from (6) into (8) and combining with (3) yields:

$$\delta LOD = \frac{LOD_o}{\Omega} \frac{\delta M_{\text{atm}}}{\bar{I}_{\text{shell}}}. \quad (9)$$

The assumptions leading to Eq. (9) imply that fluctuations in the length of day are directly proportional to fluctuations in the atmospheric angular momentum. One purpose of this thesis is to see if independent observations of  $\delta LOD$  and  $\delta M_{\text{atm}}$  are indeed related as predicted by (9).

The atmospheric angular momentum at any time can be measured by evaluating a volume integral of the east-west ( $u$ ) component of the wind from the surface of the Earth to the top of the atmosphere.

$$M_{\text{atm}} = \int_0^{2\pi} \int_{-\frac{\pi}{2}}^{\frac{\pi}{2}} \int_{r=0}^{r=\infty} \rho U(r, \phi, \theta) r^3 \cos^2(\phi) dr d\phi d\theta, \quad (10)$$

where  $r$  is distance from the center of the Earth and  $U$  is the absolute zonal velocity,  $U = r\Omega \cos \phi + u$ , and  $u$  the zonal wind. The hydrostatic relationship allows pressure coordinates to be substituted for  $\rho dr$ :

$$dr = -\frac{dp}{g\rho}. \quad (11)$$

Since the depth of the atmosphere is very small compared to the radius of the Earth,  $r$  is accurately approximated by the mean radius of the Earth,  $R_E$  ( $6.37 \times 10^6 \text{ m}$ ). With the above substitutions into (10),  $M_{\text{atm}}$  becomes:

$$M_{\text{atm}} = \frac{1}{g} \int_0^{2\pi} \int_{-\frac{\pi}{2}}^{\frac{\pi}{2}} \int_{1\text{mb}}^{\text{sfc}} (R_E \Omega \cos(\phi) + u) R_E^3 \cos^2(\phi) dp d\phi d\theta. \quad (12)$$

Separating the two parts of the integral and simplifying,

$$M_{\text{atm}} = \frac{2\pi R_E^3}{g} \int_{100\text{mb}}^{1000\text{mb}} \int_{-\frac{\pi}{2}}^{\frac{\pi}{2}} \cos^2(\phi) [u] d\phi dp \\ + \Omega \frac{R_E^4}{g} \int_0^{2\pi} \int_{-\frac{\pi}{2}}^{\frac{\pi}{2}} \cos^3(\phi) \Delta P d\phi d\theta. \quad (13)$$

The first term is the wind or motion term (Barnes *et al.* 1983). The zonal wind averaged by latitude bands is indicated by  $[u]$ . Integration limits of 100 mb and 1000 mb for the motion term were selected because the NOGAPS wind analysis extends to only 100 mb and because use of surface winds would add unnecessary complexity to the atmospheric angular momentum calculations. Since winds above 100 mb constitute less than 10% of the mass of the atmosphere, exclusion of the stratospheric winds should introduce fairly small errors. Rosen and Salstein (1985) found the stratospheric contribution to  $M_{\text{atm}}$  to be positive at semiannual periods and negative at annual periods. In other words, the stratosphere opposes the troposphere (180° out of phase) at annual cycles, and adds to tropospheric angular momentum at semiannual cycles. The amplitudes of these signals are less than 10% of the tropospheric term for annual periods, and 30% of the tropospheric term for the semiannual term. Surface winds are not used because of conflicts where surface pressure is near 1000 mb (most of the globe). In that case the near surface winds would be doubly represented.

The second term of (13) is the pressure, or matter, term (Barnes *et al.*, 1983). Most studies to date have dropped the pressure term for lack of accurate surface pressure data. Barnes *et al.* (1983) used the special observations from the GARP (Global Atmospheric Research Program) of 1979 to evaluate the pressure term and its contribution to  $M_{\text{atm}}$ . They concluded that pressure variations in  $M_{\text{atm}}$  are in phase with the wind term and fairly constant at 10% of the wind term amplitude. Indirect studies by Morgan *et al.*

(1985) show the pressure term to be 10% of the wind term at seasonal periods and no more than 25% at shorter periods.

Standard values are subtracted from  $M_{\text{atm}}$  to give  $\delta M_{\text{atm}}$ . The standard value for both the wind and pressure terms are taken to be zero. This is consistent with the atmosphere having a net angular momentum of zero with respect to the Earth. Neglecting the pressure term in (13) and using (9), changes in the Earth observed angular momentum caused by the atmosphere are:

$$\delta LOD_{\text{atm}} = \frac{LOD_o}{\Omega \bar{I}_{\text{shell}}} \frac{2\pi R_E^3}{g} \int_{100\text{mb}}^{1000\text{mb}} \int_{-\frac{\pi}{2}}^{\frac{\pi}{2}} [u] \cos^2(\phi) d\phi dp. \quad (14)$$

Eq. 14 represents the change, in units of time, that changes in the zonal wind will have on the rotation of the Earth. Thus, the independently determined measures of  $\delta LOD$  from (4) and (14) should be the same if the atmosphere is, in fact, responsible for forcing short period changes in Earth observed length of day. The data processing and the variance computations are described in the next chapter, and all of the results, implications and interpretations are given in Chapter III.



## II. DATA ACQUISITION AND PROCESSING

### A. U.S. NAVAL OBSERVATORY LOD MEASUREMENTS

Measures of  $\delta LOD$  for the period January 1983 to July 1987 were obtained from the U.S. Naval Observatory, Washington, D.C. (USNO). Included in the data set were both the Naval Observatory and the French Bureau International de l'Heure (BIH) estimates of  $\delta LOD$ . For notation purposes,  $\delta LOD_{USNO}$  will refer to the USNO data and  $\delta LOD_{BIH}$  to the French data.

### B. NOGAPS WIND DATA

Twice daily analyses of the global zonal winds for the January 1983 through August 1987 observation period were obtained from the NOGAPS model at the U.S. Navy Fleet Numerical Oceanography Center, Monterey CA. The data were in the Navy Environmental Data Network (NEDN) format. Reporting levels for the winds were standard levels plus 925 and 250mb.<sup>5</sup> The  $2\frac{1}{2}^\circ$  by  $2\frac{1}{2}^\circ$  grid produces 10,512 reporting points for the winds. A FORTRAN program was written to decode the NEDN format, manipulate the 11 by 10,512 element matrix and reduce the data to a single value of  $\delta LOD_{atm}$ . Eq. 14 was approximated by zonally averaging the matrix, integrating vertically (using a trapezoidal approximation for the unevenly spaced pressure levels), applying the  $\cos^2$  latitude terms and summing over latitude. Since the integration over latitude was performed last, the program was easily modified to get  $\delta LOD_{atm}$  values for specific latitude bands as well as the globe as a whole. Appendix A contains the source code for the program.

The archived data had few (less than 4%) missing data points. All of the missing observations in the wind data were interspersed such that linear extrapolation of the missing winds could be made. The resulting time series was smoothed with a three-day moving average filter and decimated to 1622 elements.

Similar steps were taken in determining  $\delta LOD_{atm}$  values for latitude bands within  $15^\circ$  and  $20^\circ$  of the equator, respectively. Values for the remainder of the globe were obtained by subtracting the latitude band series from the original  $\delta LOD_{atm}$  series. The

---

<sup>5</sup> Standard levels include surface, 1000, 850, 700, 500, 400, 300, 200, 150 and 100 mb. Surface winds were not used to calculate  $\delta LOD_{atm}$  because of the possible confusion with the 1000 mb winds.



purpose of the regional analysis was to investigate the possible physical mechanisms contributing to the  $LOD$  and  $M_{atm}$  relationships.

### C. ANALYSIS TECHNIQUES

Fig. 1 on page 22 shows the global  $\delta LOD_{atm}$  and the  $\delta LOD_{USNO}$  plotted together. The time data have an obvious decreasing linear trend, while the atmospheric data do not. The means of both series were removed prior to plotting. The trend in the time data is from decade fluctuations in the  $LOD$  caused by core/shell coupling (Munk and MacDonald, 1960 and Lambeck, 1980). The trend was removed by subjecting both series to a least squares algorithm found in Bendat and Piersol (1971, equation 9.20). The two detrended series are plotted in Fig. 2 on page 22. All of the series developed in the analysis were detrended with this scheme.

#### 1. Time Domain Analysis

Both series were subjected to linear filtering to isolate seasonal and subseasonal components. First, the high frequency noise and tidal oscillations were removed with a sine squared weighted moving average filter (also known as a Hanning filter) of 23 points (Fig. 3 on page 23). Weights for such a filter are determined by Robinson and Silvia, (1978):

$$W_n = \sin^2\left(\frac{\pi n}{M+1}\right) \quad n = 1, 2, 3 \dots, M, \quad (15)$$

where  $W_n$  are the filter weights and  $M$  is the total number of weights. The  $\sin^2$  weights minimize spectral distortion through unwanted side lobe leakage at the expense of a slightly smeared frequency spectrum (Robinson and Silvia, 1978). By keeping the filter symmetric, phase information of both series is preserved. Symmetric application of the filter results in the general expression of the transformed series  $y_{(t)}$  (Robinson and Silvia, 1978, Eq. 6.4):

$$y_{(t)} = \frac{2}{M-1} \sum_{i=-\frac{M-1}{2}}^{\frac{M-1}{2}} W_i x_{t-i} . \quad (16)$$

The frequency response, or convolution, of a symmetric, moving average filter of  $M$  points is given by:

$$H(f) = \frac{1}{n-1} (h_0 + 2 \sum_{l=1}^n h_l \cos(2n \pi f)), \quad (17)$$

where the series  $h$  represents the first  $(n = \frac{M+1}{2})$  weights of the symmetric series  $W_n$  and  $h_0$  is the center weight of the full series  $M$ . The term  $h_0$  will always equal one, since it is the center weight. Subtraction moving average filters have a transfer function of  $1 - H(f)$  and serve to pass high frequencies. Sine squared weights produce transfer functions almost devoid of side lobes. Plots of  $H(f)$  for each of the filters used are contained in Appendix C.

One drawback to using convolution techniques is the loss of  $M - 1$  data points (half at each end of the series) with each pass of the filter. This is particularly noticeable when using a long string of filter weights often required for lowpass systems. Nonetheless, the record length of the data (1622 points), affords sufficient length to use fairly long series of weighted moving average filters.

To isolate the seasonal terms in the  $\delta LOD_{USNO}$  and  $\delta LOD_{atm}$  series, a 75-point  $\sin^2$  weighted lowpass filter was applied twice to both series. The effect of successive filterings in the time domain is multiplication of the transfer functions in the frequency domain. The transition band with a double pass is narrower than that of a single pass. Periods less than 50 days are completely attenuated. The amplitude of annual periods are attenuated by 5% and the semiannual terms are diminished by 18%. The resulting series are plotted in Fig. 4 on page 23 and the transfer function is plotted in Fig. 18 on page 47. To further separate the seasonal terms into annual and semiannual components, both series were subjected to a 183-point unweighted moving average filter. The  $\sin^2$  weights would have required too many points to adequately filter out the semiannual terms. Using the "boxcar" unweighted filter of 183 points put the first zero at exactly the semiannual period, allowing almost complete attenuation of those signals. Disadvantages of this type of filter are the fairly large side lobes at frequencies above the first zero crossing (183 days). Since the boxcar has a fairly narrow transition band, the remaining annual terms were still about 65% of their original amplitude. The filter response is contained in Fig. 19 on page 48 in Appendix C, and the filtered series is Fig. 5 on page 24. To isolate the semiannual terms, the series obtained from the 183-point boxcar filter was subtracted from the twice run 75-point weighted series. The resulting semiannual

series was attenuated less than 15% at periods of 200 days. Response for this series is contained in Fig. 20 on page 48.

Oscillations with periods from 20 to 100 (subseasonal) days were isolated with high and lowpass filters. The highpass filter consisted of two passes of a subtracted moving average of 75 points. Lowpass was achieved with a single run of a 23-point weighted moving average filter. The resulting series are plotted in Fig. 7 on page 25. Fig. 21 in Appendix C contains the frequency response of the filter.

For latitude band comparisons, the  $\delta LOD_{USNO}$  series was separated into relatively high frequency (subseasonal) and relatively low frequency (seasonal) components. The transition band was from  $1/60 \text{ day}^{-1}$  to  $1/150 \text{ day}^{-1}$ . These two series (heavy lines in Figs. 4 and 7),  $\delta LOD_{USNO\text{-}seasonal}$  and  $\delta LOD_{USNO\text{-}subseas}$ , were then individually compared to the corresponding  $\delta LOD_{atm}$  time series generated from tropical and extratropical zonal winds. These plots are contained in Figs. 8 through 11. Naming conventions for these series are:

- $\delta LOD_{USNO\text{-}seasonal}$ : Seasonal (150 to 365 day periods) values of USNO determined  $\delta LOD$ .
- $\delta LOD_{USNO\text{-}subseas}$ : Subseasonal (20 to 100 day periods) values of USNO determined  $\delta LOD$ .
- $\delta LOD_{atm15}$ : Atmospherically derived  $\delta LOD$  from  $15^{\circ}N$  to  $15^{\circ}S$ .
- $\delta LOD_{atm\sim S}$ : Atmospherically derived  $\delta LOD$  from  $15^{\circ}N$  to the North Pole and  $15^{\circ}S$  to the South Pole.
- $\delta LOD_{atm20}$  and  $\delta LOD_{atm70}$ : Atmospherically derived  $\delta LOD$  with cutoff at  $20^{\circ}N$  and  $S$ .

## 2. Frequency Domain Analysis

Prior to Fourier analysis, each series was tapered with a cosine bell to reduce leakage at the ends of the time series data. Both series were extended to a length of 2048 points by the addition of zeros to each end of the record. The effects of the tapering were removed after the transform by dividing each element by the ratio of the area of the taper (the cosine) to the rectangular boxcar area replaced by the taper; a factor of 0.875 (Bendat and Piersol, 1971).

A record length of 2048 permitted the use of the Fast Fourier Transform (FFT) algorithm (Bendat and Piersol, 1971), significantly cutting down the computation time required for the transforms. After transforming, the complex valued cross spectral am-



plitude coefficients were determined from the complex amplitude coefficients of the time and atmospheric series ( $X_{(n)}$  and  $Y_{(n)}$ ). Cross spectral coefficients are:

$$XY_{(n)} = \frac{2X_{(n)}^* Y_{(n)}}{\Delta f} \quad n = 0, 1, 2, \dots, \frac{N}{2}, \quad (18)$$

where  $n$  represents the index number of the  $\frac{N}{2} + 1$  resolvable frequencies from a sample size of  $N$  and  $X^*$  is the complex conjugate of  $X$ . The three complex valued series,  $X$ ,  $Y$ , and,  $XY$ , were then smoothed in order to increase the confidence intervals of the power spectral density functions as well as the coherence squared ( $\gamma^2$ ) and phase ( $\phi$ ) functions. Prior to smoothing, the spectral estimates were prewhitened by multiplication by the square of the frequency at each estimate. Jenkins and Watt (1968) state that estimates of coherency and phase should be based on white spectra. This technique (also used by Eubanks *et al.*, 1985), compensates for the  $f^{-2}$  power law followed by both the time and atmospheric data. The complex spectral and co-spectral estimates were smoothed with a seven-point unweighted moving average to give 14 degrees of freedom for calculating confidence and significance intervals. Energy density estimates were formed by taking the magnitude of the complex coefficients:

$$\hat{G}_x = \frac{2|X_{(n)}|^2}{\Delta f} \quad ; \quad \hat{G}_y = \frac{2|Y_{(n)}|^2}{\Delta f}. \quad (19)$$

Coherence squared is defined as:

$$\hat{\gamma}^2 = \frac{|X_{(n)}^* Y_{(n)}|^2}{\hat{G}_x(n)\hat{G}_y(n)}. \quad (20)$$

Phase is determined by:

$$\phi = \tan^{-1} \frac{\text{Im}[X_{(n)}^* Y_{(n)}]}{\text{Real}[X_{(n)}^* Y_{(n)}]}. \quad (21)$$

Eqs. 19, 20 and 21 were calculated and plotted for the  $\delta LOD_{USNO}$  and  $\delta LOD_{atm}$  series, as well as the tropical and extratropical  $\delta LOD_{atm}$  series against the  $\delta LOD_{USNO}$ . Figs. 12 through 16 are the plots for these series.

### 3. Harmonic Analysis

For comparison with earlier findings of Rosen and Salstein (1985), Morgan *et al.* (1985), and Langley *et al.* (1981), a harmonic analysis was performed to obtain the annual and semiannual terms of both time and atmospheric signals. The Fourier analysis was done for the three calendar years for which the data were continuous: 1984, 1985 and 1986. Phase and amplitude were determined from the sine and cosine sums of:

$$A_{(i) \sin} = \frac{2}{365} \int_0^{365} X(t) \sin(2\pi f_i t) dt; \quad A_{(i) \cos} = \frac{2}{365} \int_0^{365} X(t) \cos(2\pi f_i t) dt, \quad (22)$$

where  $f_i$  is the frequency of interest ( $1/365 \text{ day}^{-1}$  and  $1/182.5 \text{ day}^{-1}$ ) and  $t$  is the integer time in days from the beginning to the end of the year. Amplitude for the frequencies is  $\sqrt{A_{i \cos}^2 + A_{i \sin}^2}$  and phase is  $\tan^{-1}(A_{i \sin}/A_{i \cos})$  converted to days from 1 January of that year. Results and comparisons with earlier findings are in Table 3.

### III. RESULTS

#### A. GLOBAL COMPARISON IN THE TIME DOMAIN

The detrended  $\delta LOD_{USNO}$  and  $\delta LOD_{atm}$  series (Figs. 2 and 3) match fairly closely. The linear correlation coefficient for the two series with tides and high frequency noise removed is 0.990.<sup>6</sup> From Fig. 2 on page 22 it can be seen that the signals with the longer periods have larger amplitudes. This is the time domain analogy of the  $f^{-2}$  relationship found in the spectra of  $\delta LOD_{USNO}$  and  $\delta LOD_{atm}$ . The lowest period that correlation can be expected is around 20 days because the 23-point filter used to smooth the data completely removes periods of 15 days or less. Additionally, contamination from the unwanted tidal signal at a period of 13 days would make correlation at or near that period impossible.

##### 1. Seasonal Components

Seasonal variations stand out, with the largest values of both  $\delta LOD_{USNO}$  and  $\delta LOD_{atm}$  occurring in January and July. Munk and MacDonald (1960) observed these seasonal effects, and also noted that the amplitudes of the annual oscillations were greater in July than in January. This corresponds to the uneven contribution (by almost a factor of two in Munk and MacDonald's computations) of the two hemispheres to the angular momentum budget during January and July. Thus, a typical day in January is almost one millisecond longer than a typical day in July. In January, strong westerlies from the winter (northern) hemisphere dominate the global angular momentum and cause the observed decrease in the length of day. In other words, the Earth spins slower because the atmosphere is spinning faster. In July, the upper level westerlies in the northern hemisphere are weakened by the breakdown of the midlatitude baroclinic zone. Meanwhile, the southern hemisphere, because of its smaller land mass, does not compensate with stronger westerlies. The net effect is for a minimum of atmospheric angular momentum in July and a corresponding maximum in Earth rotation rate, and the reverse in January; maximum angular momentum and minimum earth rotation rate.

---

<sup>6</sup> The linear correlation coefficient is defined as  $\rho_{xy} = \text{Cov}_{xy}/\sigma_x\sigma_y$ . Its analogy in frequency space is coherence, although the coherence statistic used in this paper is more properly called coherence squared ( $\gamma^2$ ); see Eq. (20). Direct comparisons of the two statistics,  $\gamma^2$  and  $\rho$ , is of qualitative value only because  $\gamma^2$  is frequency dependent while  $\rho_{xy}$  is not.



The seasonal components of  $\delta LOD_{\text{USNO}}$  and  $\delta LOD_{\text{atm}}$  (Fig. 4 on page 23) appear to be two in-phase sinusoids of annual and semiannual frequency. The linear correlation, 0.990, is significantly higher than the subseasonal linear correlation of 0.853 (refer to Table 1). The  $\delta LOD_{\text{USNO}}$  has slightly greater amplitude, shown by its greater variance (Table 1). Since a fundamental assumption (made earlier) is that the  $\delta LOD_{\text{USNO}}$  signal represents the total of all atmospheric (as well as other, unmodelled, sources of) angular momentum, it is not surprising that the seasonal terms of the atmosphere are less than the time signals. The neglected pressure term in (13), oceanic currents, and stratospheric winds are probably the missing inputs to balance the seasonal terms. Of particular note is the difference in amplitudes found in mid July of 1984 and 1986. The Quasi-Biennial-Oscillation (QBO) peaked at exactly those two times (R.A. Madden, personal communication, 1988). The peak was for easterly stratospheric winds; enough to qualitatively account for the significant amplitude difference of the troposphere and measured  $LOD$ .

Figs. 5 and 6 are the decompositions of the seasonal signals depicted in Fig. 4 on page 23 into annual and semiannual parts. Annual terms, Fig. 5 on page 24, appear smaller than those determined by harmonic analysis (Table 3) because the filter transfer function (required to separate the closely spaced annual and semiannual terms) attenuated the annual signal 65%. Fig. 19 in Appendix C is the plot of the spectral response of the filter used to isolate these terms. Residuals of  $\delta LOD_{\text{USNO}}$  and  $\delta LOD_{\text{atm}}$  show a small biannual bias which is probably associated with the QBO.

Fig. 6 on page 24 contains the semiannual part of the seasonal signal. The spectral response of the filtering (Fig. 20, Appendix C) show minimal amplitude losses due to the filtering process. The amplitude from the plot, about 0.3 ms, agrees well with the harmonic analysis (Table 3) and with the findings of Rosen and Salstein (1985). These data show, as other data have in previous studies, that variations in the length of the day on seasonal timescales (annual and semiannual periods) are almost entirely due to meteorological influences.

## 2. Subseasonal Components

Subseasonal is defined to include periods from 20 to 150 days. Fig. 7 on page 25 shows the close match of the subseasonal signals in both phase and amplitude. The correlation coefficient of the two series is 0.853. The high peaks are associated with periods around 50 days while the lower peaks correspond to shorter periods, as is expected with the  $f^{-2}$  power spectrum discussed earlier. The 50-day peaks are perhaps associated

with the 40-50 day oscillations in the tropics first described by Madden and Julian (1971). The average amplitude of 0.25 ms is slightly larger than that found by Eubanks *et al.* (1985) for the period 1977-1981, and agree well with the findings of Morgan *et al.* (1985) for the period 1981-1983.

## B. GLOBAL COMPARISONS IN THE FREQUENCY DOMAIN

### 1. The Energy Density Spectra of $\delta LOD_{\text{atm}}$ and $\delta LOD_{\text{USNO}}$

Plots of  $\delta LOD_{\text{USNO}}$  and  $\delta LOD_{\text{atm}}$  energy density, coherence and phase are contained in Fig. 12 on page 28. The most striking feature of the energy density plot is the large peaks at annual and semiannual periods. This is consistent with the largest amplitude oscillations in the time domain (Fig. 2 on page 22) occurring seasonally. Also noteworthy are the sharp spikes at periods of 13 and seven days in the  $\delta LOD_{\text{USNO}}$  spectrum. These are high frequency tidal oscillations which were not filtered out of the original time data.

The slope of both spectra is -2 (indicated by the sloping double line on the energy density plot). Eubanks *et al.* (1985), state that, while the cause of the  $f^{-2}$  dependence in the power spectrum is not clear, it shows up in a wide variety of geophysical phenomena. Near the Nyquist frequency of  $.5 \text{ day}^{-1}$ , the  $\delta LOD_{\text{USNO}}$  spectrum falls off at a more rapid rate than expected by the  $f^{-2}$  relationship. This is an indication of the lower noise level of the  $\delta LOD_{\text{USNO}}$  data. Eubanks *et al.* (1985) experiments were conducted prior to recent advances in more accurate astronomic LOD measurements; thus their data probably have a somewhat noisier spectrum at higher frequencies (personal communication with J.O. Dickey, co-author with Eubanks *et al.*, 1985).

At periods of 16 days and greater, the two spectra are in agreement. In addition to the broad peaks at annual and semiannual periods, there are broad peaks at 75 and 50 days, and narrower peaks at 33 and 25 days.

### 2. Coherence Spectrum

The coherence spectrum in Fig. 12 shows strong coherence (or correlation) at seasonal as well as periods centered around 75, 50, 33, 25 and 20 days. As would be expected, these periods show corresponding power in the energy density plots. The 95% confidence line in the coherence plot is derived from a 95% significance level in rejecting a null hypothesis of no coherence between the two series. The coherence plot agrees well with that of Eubanks *et al.* (1985). Of note is the rapid drop off in coherence at periods around 125 days (also found by Eubanks *et al.* 1985). This may be related to a general lack of power in both the  $\delta LOD_{\text{atm}}$  and  $\delta LOD_{\text{USNO}}$  spectra, however, the loss of



power does not completely explain the steep drop in coherence. It is possible that whatever (weak) oscillations there are in the length of day at periods around 125 days, they are not of meteorological origin. Significant coherence at periods as low as 20 days indicates that the atmosphere can generate short period, high frequency, changes in the  $LOD$ . Given accurate enough time and wind data, fluctuations of even one or two day time scales will eventually be resolved (Lambeck, 1980).

### 3. Phase Spectrum

The phase plot shows that, except for a small spike at 125 days, changes of  $\delta LOD_{atm}$  and  $\delta LOD_{USNO}$  occur within five days of each other. Generally, phase is closest to zero where coherence is highest, indicating changes in angular momentum are rapidly transmitted between Earth and atmosphere. Measurements of atmospheric angular momentum in this study cannot readily be decomposed into specific torques responsible for transfer of momentum. Swinbank (1985) found that shorter period fluctuations (from daily to subseasonal) result from mountain torques (pressure differences across north/south oriented mountain ranges) and seasonal variations result from friction torques (frictional drag at the surface boundary layer of the Earth and atmosphere).

### 4. Harmonic Analysis

Amplitude and phase information of the first two harmonic frequencies of  $\delta LOD_{USNO}$  and  $\delta LOD_{atm}$  were calculated by year. The results (Table 3) compare favorably with previous studies (Morgan *et al.*, 1985, and Rosen and Salstein, 1985), although the annual amplitudes found in this study show more variability than those found in the previously cited studies. Of note is the two-month variation in phases (Jan-Feb for annual terms and May-Jun for semiannual terms).

## C. LATITUDE COMPARISONS OF LOD

Comparisons of  $\delta LOD_{USNO}$  with tropical and extratropical partitions of  $\delta LOD_{atm}$  are shown in Figs. 13 through 16. As noted above, the reason for computing  $\delta LOD_{atm}$  over specific latitude bands (equatorial and extratropical regions, respectively) is to try to identify the particular geographical region that is contributing to the high coherence between  $\delta LOD_{atm}$  and  $\delta LOD_{USNO}$ . Energy density plots show significant drops in power at periods between one year and 30 days for the extratropical,  $\delta LOD_{atm75}$  and  $\delta LOD_{atm70}$ , series. The two tropical series, ( $\delta LOD_{atm15}$  and  $\delta LOD_{atm20}$ ) show power losses only at periods longer than 100 days. Coherence for the extratropical series dropped below 0.5 for most periods between 30 and 100 days; for the tropical series, coherence at these periods dropped only slightly. Coherence falls off rapidly in both tropical and extratropical series

around periods of 125 days. The extratropical series fall to near zero at these periods. This may be related to the local minimum of power at periods from 80 to 125 days in all atmospheric and USNO energy density plots. The phase plots show that at the annual period, changes in the atmosphere tend to lead changes in the length of day in extratropical latitudes (Fig. 14 and especially 16) while they tend to lag changes in the length of day in the equatorial regions. This simply reflects the fact that the annual cycle in the equatorial region is shifted or delayed somewhat in time relative to the middle latitudes.

At subseasonal periods, it is very difficult to interpret much about the geographical origin of events with periods shorter than about 30 days. The generally high power and coherence near 20-30 days in Fig. 12 does not seem to be of only equatorial or only midlatitude origin. However, the evidence very clearly indicates that the tropics and equatorial regions are responsible for most of the fluctuations of  $\delta LOD$  in the 40-to 100-day range. Thus, the high power and coherence at 50-60 day and at 70-100 day periods in Fig. 12 also appear in Figs. 13 and 15 (using only tropical wind data), but they are completely absent in Figs. 14 and 16 where only extratropical wind data were used in computing  $\delta LOD_{atm}$ . The dividing line between the tropical and extratropical regions is not very clear because only two latitude bands have been considered. Also, seasonal signals are still apparent in the tropical regions, and, to a lesser degree, subseasonal (40-to 100-day periods) oscillations are seen outside the tropics.

#### IV. SUMMARY

It is clear that changes in atmospheric angular momentum can account for the vast majority of short period (one year or less) changes in the  $LOD$ . Time and frequency domain analyses show that over 90% of the variance in seasonal and subseasonal periods of  $\delta LOD_{atm}$  is explained by  $\delta LOD_{USNO}$ . Meteorological activity is responsible for all changes in  $LOD$  within present measurement capabilities. While error analysis of the atmospheric and time series is beyond the scope of this paper, Morgan *et al.* (1985) accounted for most of the variances between the series as being within measurement limits. In addition, Rosen and Salstein (1985) reduced the variance due to unknown sources to less than  $0.04 \text{ (ms)}^2$  for annual and  $0.03 \text{ (ms)}^2$  for semiannual terms (measured in units of amplitude). Phase differences between  $\delta LOD_{atm}$  and  $\delta LOD_{USNO}$  are very near zero, indicating that an almost instantaneous transfer of angular momentum occurs between Earth and the atmosphere. Additionally, when the pressure term is included, an rms error of less than  $0.25 \text{ (ms)}^2$  at seasonal periods results (Barnes *et al.*, 1983). Other studies (Eubanks *et al.*, 1985 and 1986), conclude that measurement errors exceed the unexplained variance of  $\delta LOD$ .

The value of establishing the strong coherence and correlation of the independently measured signals of  $\delta LOD_{atm}$  and  $\delta LOD_{USNO}$  include:

- Astronomic measures of  $LOD$  can be used as an independent measure of the state of the zonal atmospheric winds. Analysis and forecasting models can use this as a check of data consistency.
- Rapid changes of  $LOD$ , such as were observed in the El Nino event of 1983, can perhaps be used to infer future El Nino events (Eubanks *et al.* 1986, and Rosen *et al.* 1984). Other weather phenomena with a strong zonal component, such as the 40-50 day tropical oscillations, can be temporally located by real time filtering and analysis of  $\delta LOD_{atm}$  data.
- Dickey *et al.* (1986) reported that atmospheric angular momentum can be used to infer real time  $\delta LOD$ . This is required for extremely precise Earth position fixes to navigate spacecraft. Real time calculations of atmospheric angular momentum and  $\delta LOD_{atm}$  are currently computed and archived by NMC.

The findings of this paper are in agreement with previous studies. The finer resolution of the USNO time data beginning in 1983 (the BIH time data also had similar improvements starting in 1983) shows that atmospherically and astronomically derived



$\delta LOD$  are coherent down to periods of 20 days or less. The NOGAPS wind analyses compare well with similar studies done with NMC or ECMWF.

Comparing latitude bands of integrated  $\delta LOD_{\text{atm}}$  with  $\delta LOD_{\text{USNO}}$  confirms that there is spatial variability in both phase and amplitude of atmospheric angular momentum. Seasonal changes at annual periods of  $\delta LOD$  appear to originate primarily in the extratropical regions. Subseasonal fluctuations (30-100 day periods) in  $\delta LOD_{\text{atm}}$  have significantly more amplitude (power) and coherence with  $\delta LOD_{\text{USNO}}$  when computed from tropical data than extratropical data. This strongly suggests that changes in the length of day at these time scales is produced by meteorological events in the tropics- *e.g.* the 30-60 day oscillations of Madden and Julian (1971, 1972). Further study, including more latitude band divisions of the globe is required to be more exact on the position of the dividing line between the tropics and extratropics. This study indicates that the latitude band responsible for most of the subseasonal fluctuations of the length of the day is approximately  $20^{\circ}\text{N}$  to  $20^{\circ}\text{S}$ .

**Table 1. LINEAR CORRELATION COEFFICIENTS**

	$\delta LOD_{\text{atm}}$	$\delta LOD_{\text{atm-seasonal}}$	$\delta LOD_{\text{atm-subseas}}$	$\delta LOD_{\text{atm15}}$	$\delta LOD_{\text{atm75}}$	$\delta LOD_{\text{atm20}}$	$\delta LOD_{\text{atm70}}$
$\delta LOD_{\text{USNO}}$	.990						
$\delta LOD_{\text{USNO-seasonal}}$	.990	.938		.664	.872	.691	.872
$\delta LOD_{\text{USNO-subseas}}$	.623		.853	.599	.488	.595	.477

**Table 2. VARIANCES**

$\delta LOD_{USNO}$	.148
$\delta LOD_{USNO\text{-}seasonal}$	.114
$\delta LOD_{USNO\text{-}subseas}$	.013
$\delta LOD_{atm}$	.134
$\delta LOD_{atm\text{-}seasonal}$	.089
$\delta LOD_{atm\text{-}subseas}$	.011
$\delta LOD_{atm15}$	.044
$\delta LOD_{atm75}$	.046
$\delta LOD_{atm20}$	.074
$\delta LOD_{atm70}$	.046
all values in (ms) <sup>2</sup>	

**Table 3. PHASE AND AMPLITUDES OF LOD**

		Annual		Semiannual	
		amplitude <sup>1</sup>	phase <sup>2</sup>	amplitude	phase
$\delta LOD_{USNO}$	1984	0.290	Jan 14	0.205	May 15
$\delta LOD_{atm}$	1984	0.269	Jan 12	0.223	May 10
$\delta LOD_{USNO}$	1985	0.434	Feb 25	0.366	Jun 10
$\delta LOD_{atm}$	1985	0.469	Feb 28	0.359	Jun 11
$\delta LOD_{USNO}$	1986	0.304	Feb 1	0.225	May 9
$\delta LOD_{atm}$	1986	0.230	Feb 2	0.226	May 12
$\delta LOD_{BIH}^3$	1980-1981	0.367	Feb 6-8	0.273	May 7-9
$\delta LOD_{NMC}^3$	1980-1981	0.363	Feb 4	0.282	May 13
$\delta LOD_{UT1}^4$	1981-1983	0.45	Feb 16	0.24	May 1
$\delta LOD_{NMC}^4$	1981-1983	0.50	Feb 12	0.17	May 1

Note 1. Amplitude is in ms.

Note 2. Phase is the peak value of that term in days starting with Jan 1.  
For the semiannual phase, the date is the day of the first peak in the year.

Note 3. From Rosen and Salstein (1985). Time data is from BIH. NMC weather data extends to 1 mb.

Note 4. From Morgan *et al.* (1985). Time data is a composite of LLR, VLBI, and BIH estimates. NMC data extends to 100 mb.

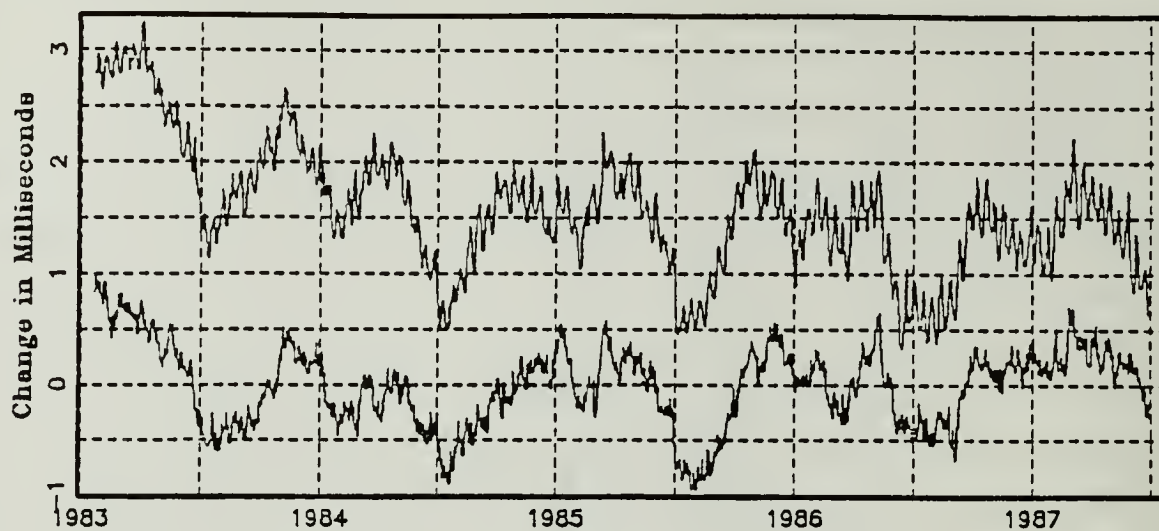


Fig. 1. Unfiltered time series of  $\delta LOD_{USNO}$  (top) and  $\delta LOD_{atm}$  (bottom): Note the linear, decreasing trend in the  $\delta LOD_{USNO}$  plot. The mean has not been removed from the USNO data.

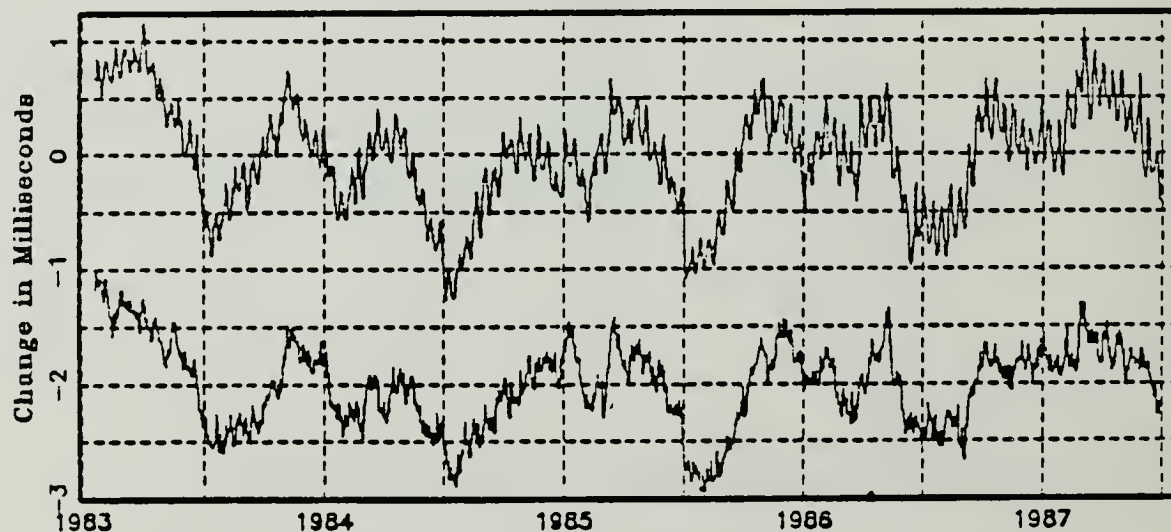


Fig. 2. Detrended  $\delta LOD_{atm}$  and  $\delta LOD_{USNO}$  series: Top line is USNO data. Bottom line (atmospheric data) has been offset by -0.2 ms for clarity

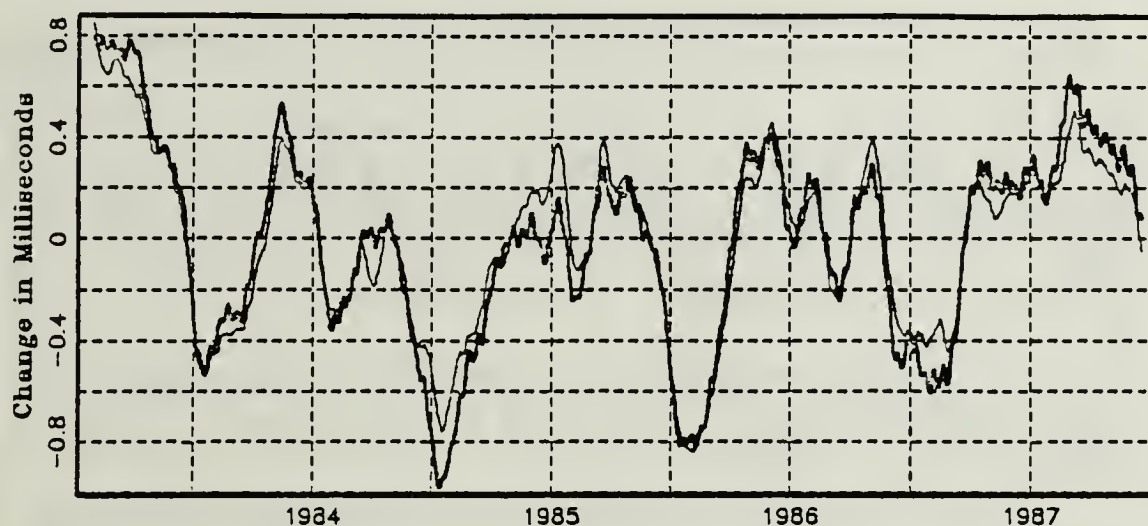


Fig. 3. Smoothed  $\delta LOD_{atm}$  and  $\delta LOD_{USNO}$  series: A 23-point moving average filter was used to eliminate noise and high frequency tidal oscillations. Heavy line is the  $\delta LOD_{USNO}$  series.

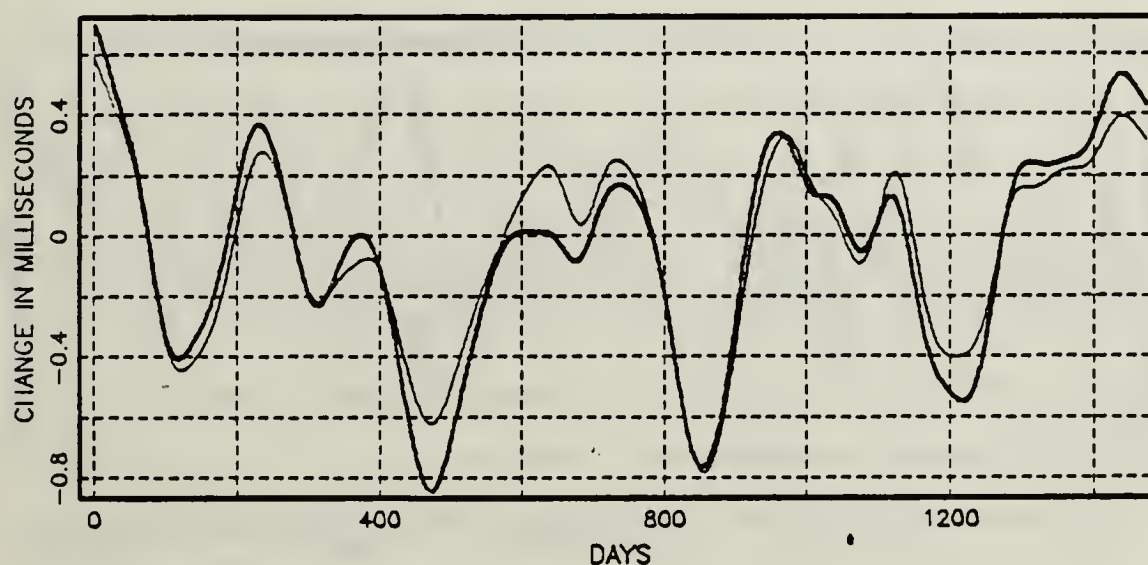


Fig. 4. Seasonal terms of  $\delta LOD_{atm}$  and  $\delta LOD_{USNO}$ : Heavy line is USNO series. A 75-point weighted moving average filter was applied twice to each series; 148 points were lost from the ends.



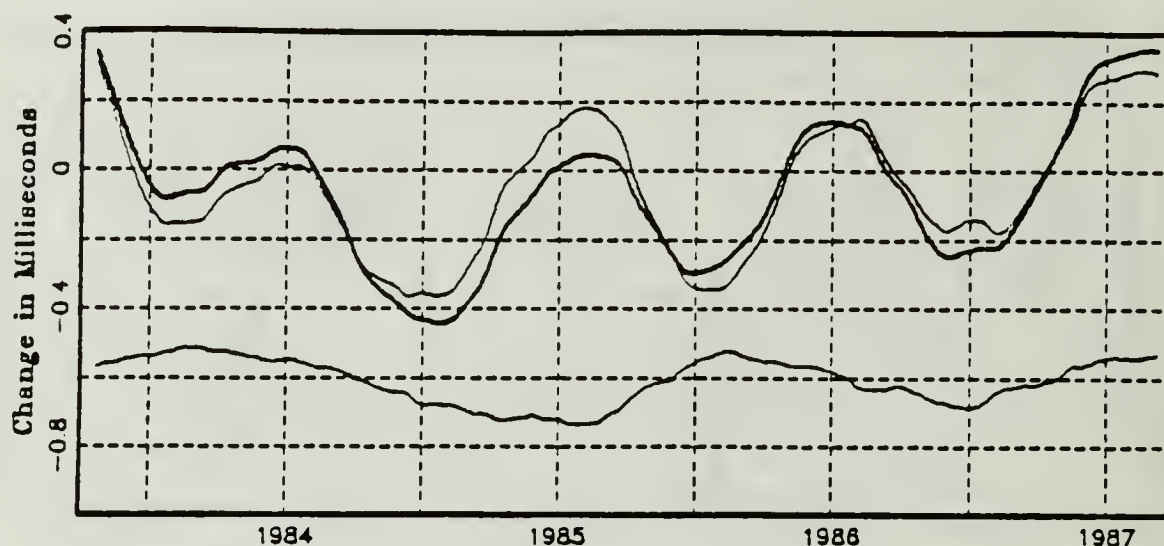


Fig. 5. Annual terms of  $\delta LOD_{USNO}$  and  $\delta LOD_{atm}$ : Heavy line is  $\delta LOD_{USNO}$ . Bottom graph is residual of  $\delta LOD_{USNO} - \delta LOD_{atm}$  shifted downward by 0.2 ms. The slight oscillation of this line is at a period of 2 years and is probably related to the Quasi-Biennial-Oscillation. Frequency transfer function is Fig. 19 on page 48 of Appendix C.

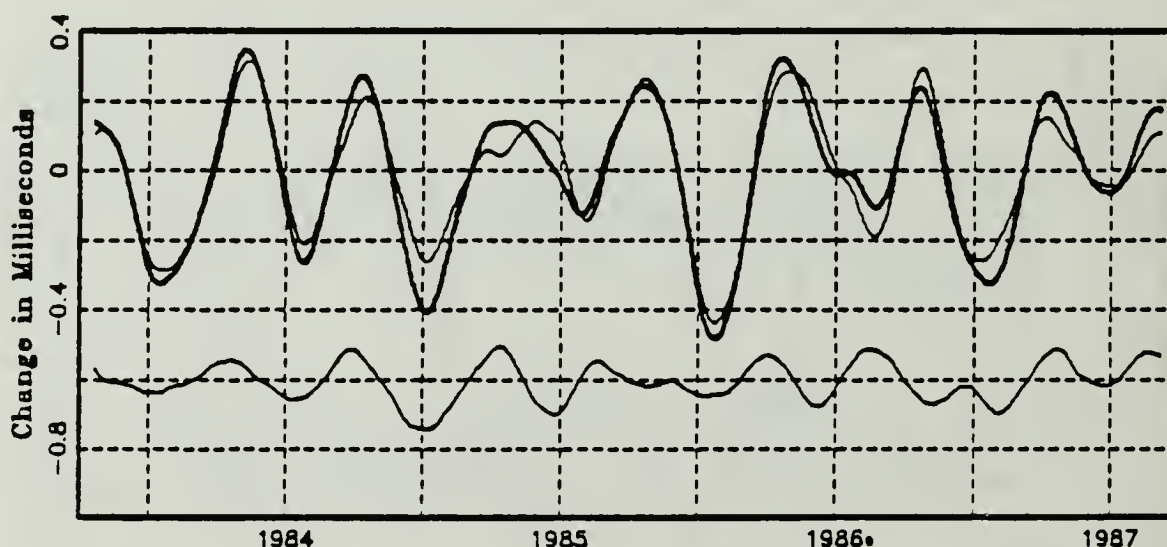


Fig. 6. Semiannual terms of  $\delta LOD_{USNO}$  and  $\delta LOD_{atm}$ : Heavy line is  $\delta LOD_{USNO}$ . Bottom graph is residual of  $\delta LOD_{USNO} - \delta LOD_{atm}$  shifted down by 0.5 ms. Frequency response of filter is Fig. 20 on page 48 of Appendix C.



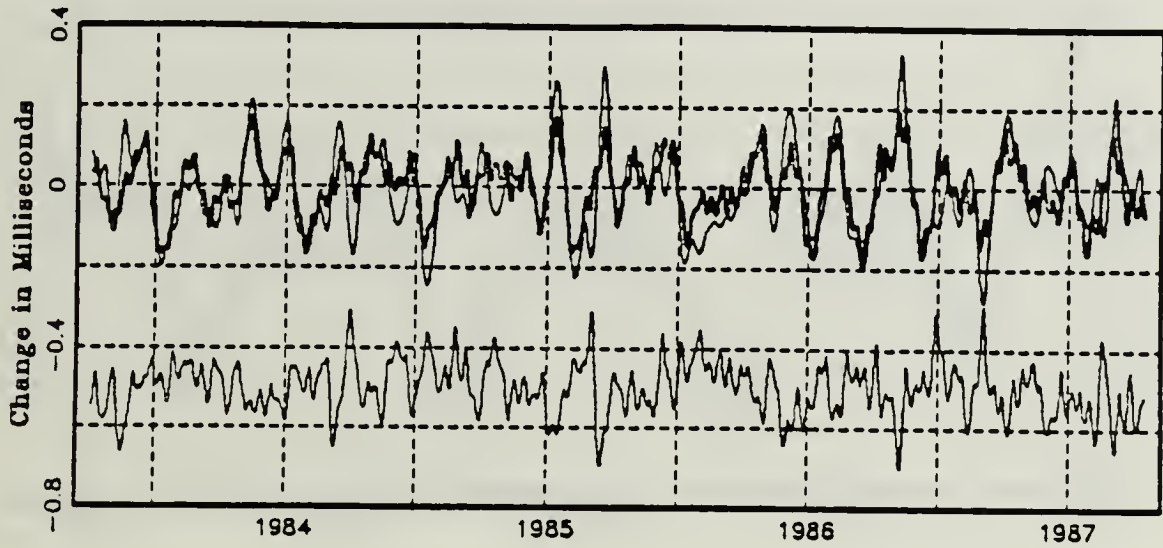


Fig. 7. Subseasonal Oscillations of  $\delta LOD_{atm}$  and  $\delta LOD_{USNO}$ : Residual of series depicted in Fig. 4 on page 23 subtracted from Fig. 3 on page 23. Bottom line is the difference of the two series shifted down 0.5 ms.

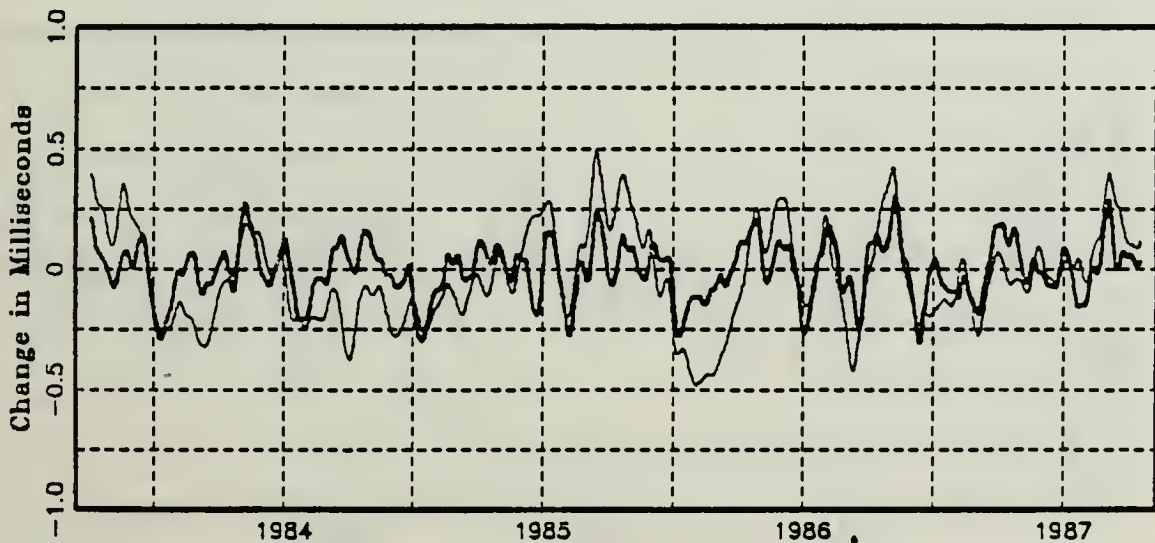


Fig. 8. Comparison of  $\delta LOD_{USNO-subseason}$  and  $\delta LOD_{atm15}$ : Heavy line is  $\delta LOD_{USNO}$  seasonal signal; light line is  $\delta LOD_{atm15}$  derived from integrating atmospheric angular momentum within  $15^\circ$  of the equator.

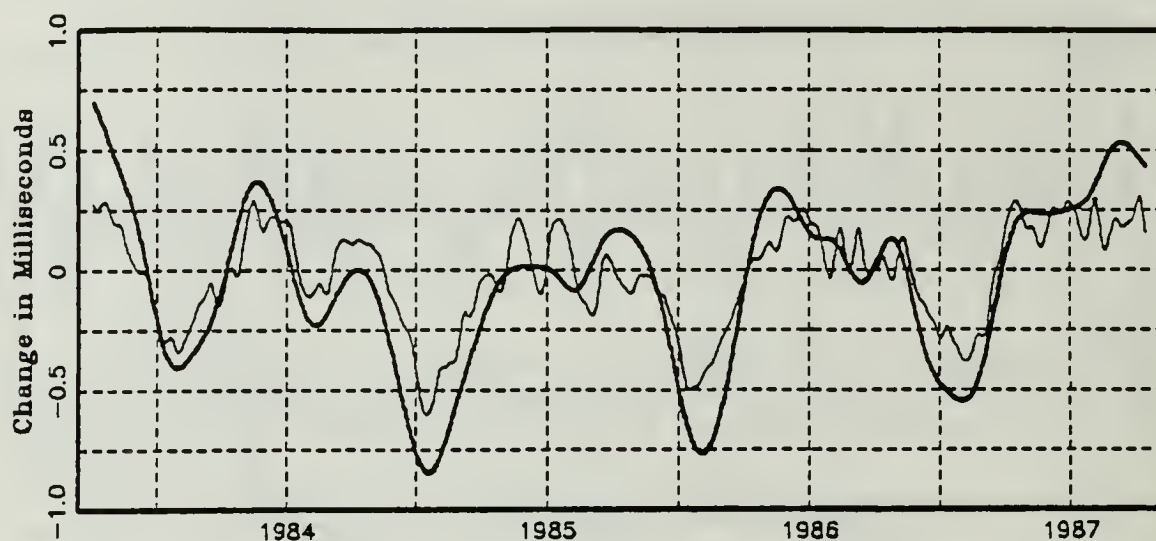


Fig. 9. Comparison of  $\delta LOD_{USNO\text{-}seasonal}$  and  $\delta LOD_{atm75}$ : Same as Fig. 8, except midlatitude components poleward of  $15^\circ N$  and  $15^\circ S$  are compared with seasonal terms of  $\delta LOD_{USNO}$ .

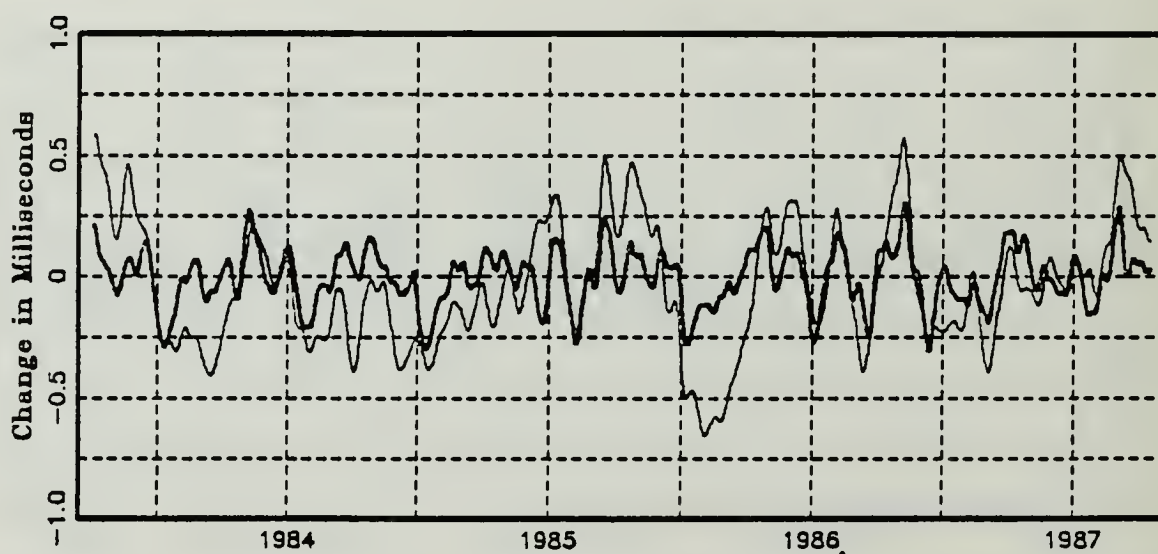


Fig. 10. Comparison of  $\delta LOD_{USNO\text{-}subseas}$  and  $\delta LOD_{atm20}$ : Heavy line is USNO subseasonal signal (from Fig. 7); light line is derived from integrating atmospheric angular momentum within  $20^\circ$  of the equator.

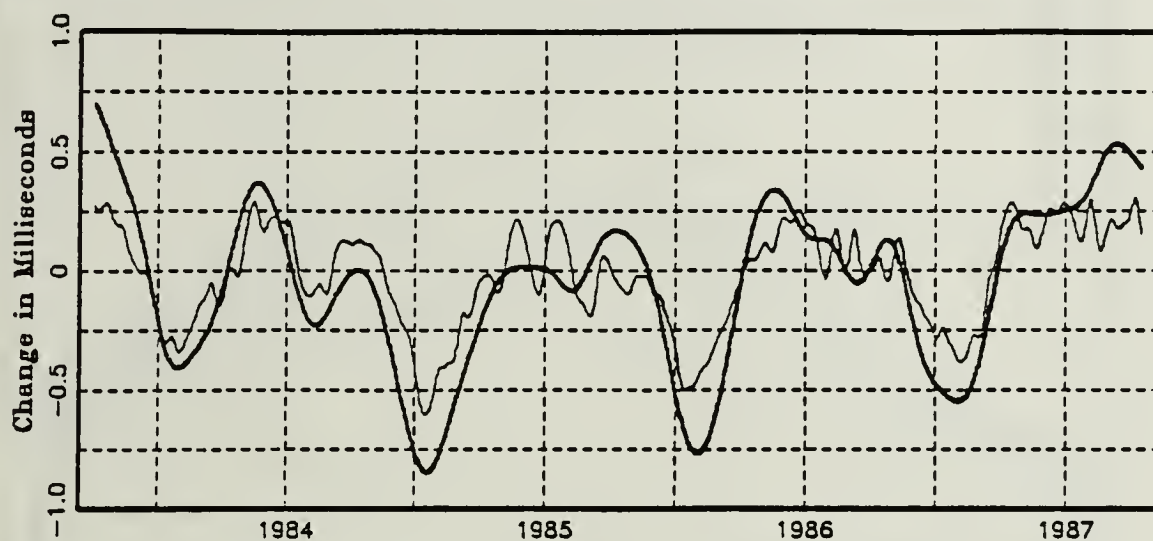


Fig. 11. Comparison of  $\delta LOD_{\text{USNO-seasonal}}$  and  $\delta LOD_{\text{atm70}}$ : Heavy line is USNO seasonal signal (from Fig. 6); light line is atmospheric signal derived from midlatitude components of atmospheric  $LOD$  above  $20^\circ N$  and below  $20^\circ S$ .

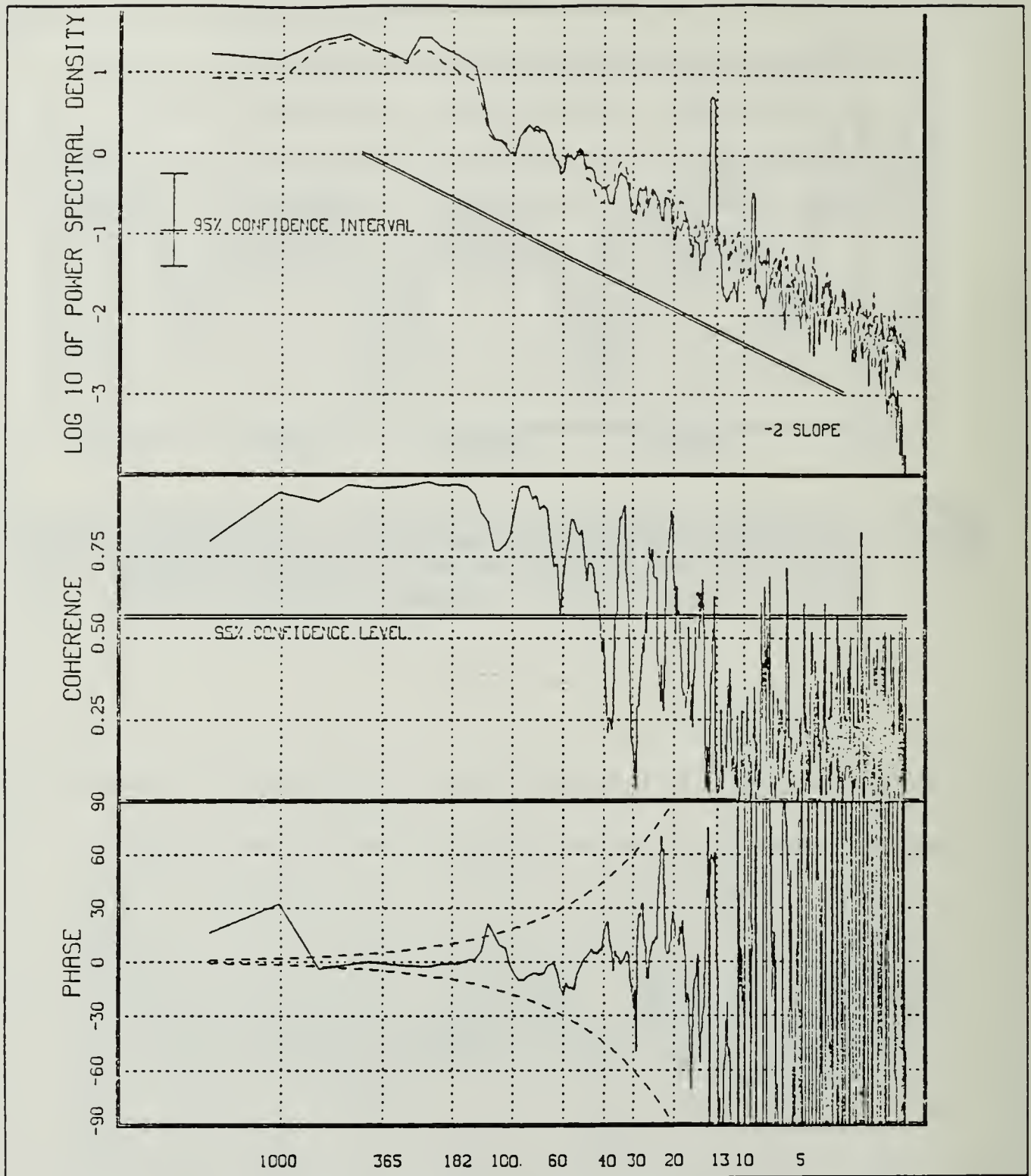


Fig. 12. Energy Density, Coherence, and Phase Spectra of  $\delta LOD_{atm}$  and  $\delta LOD_{USNO}$ : Seven point spectral smoothing used for all plots. Solid line in the power spectral density spectral plot is  $\delta LOD_{USNO}$  and dashed line is  $\delta LOD_{atm}$ . Dashed lines in phase plot are 5 day advances (top dashed line) and lags (bottom dashed line) of  $\delta LOD_{USNO}$  with respect to  $\delta LOD_{atm}$ . Horizontal line in coherence plot represents 95% confidence that the two series are correlated.



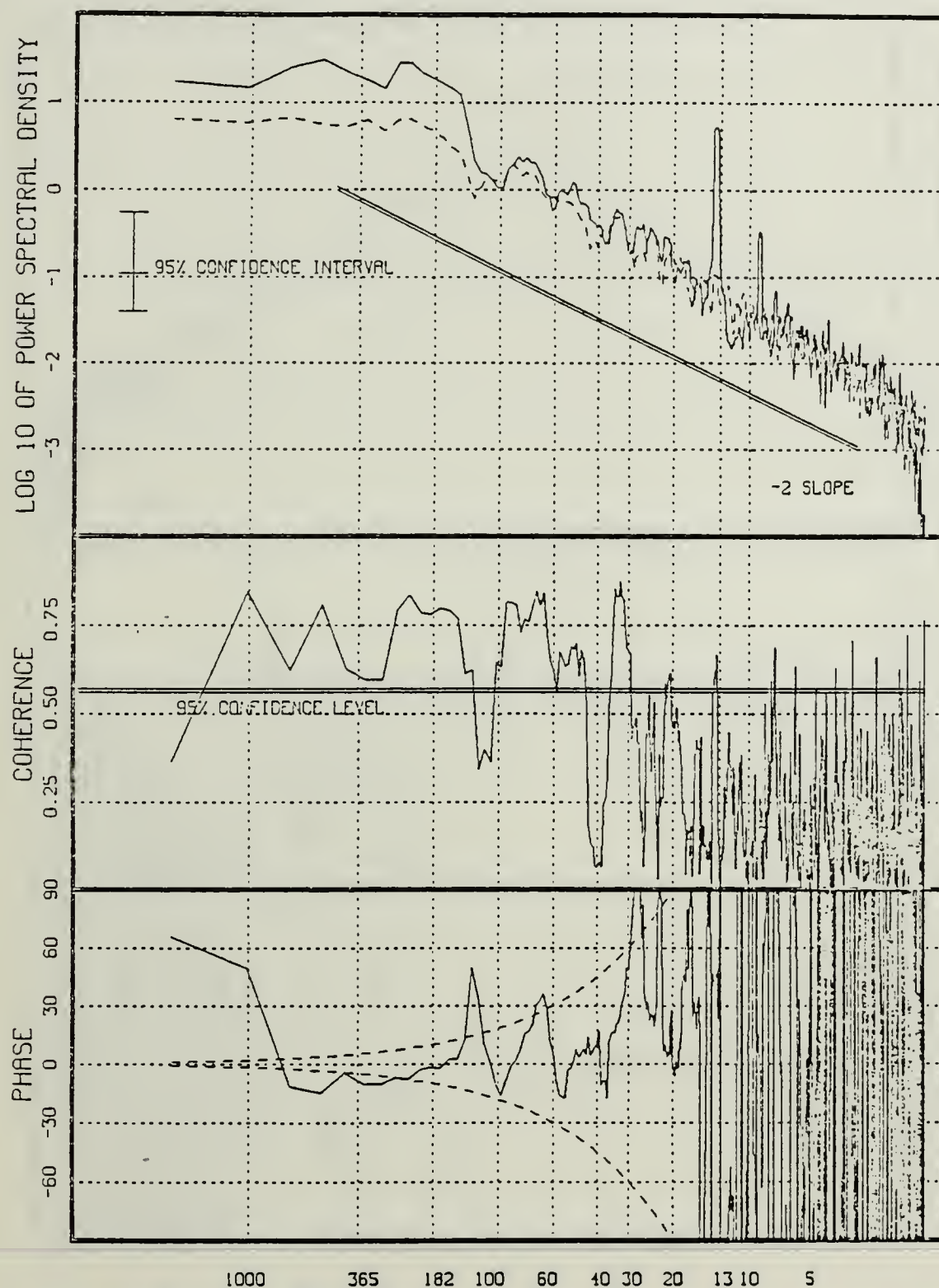


Fig. 13. Energy Density, Coherence, and Phase Spectra of  $\delta LOD_{USNO}$  and  $\delta LOD_{atm15^\circ}$ : As in Fig. 12 except the atmospheric signal is  $\delta LOD_{atm}$  computed within  $15^\circ$  of the equator.



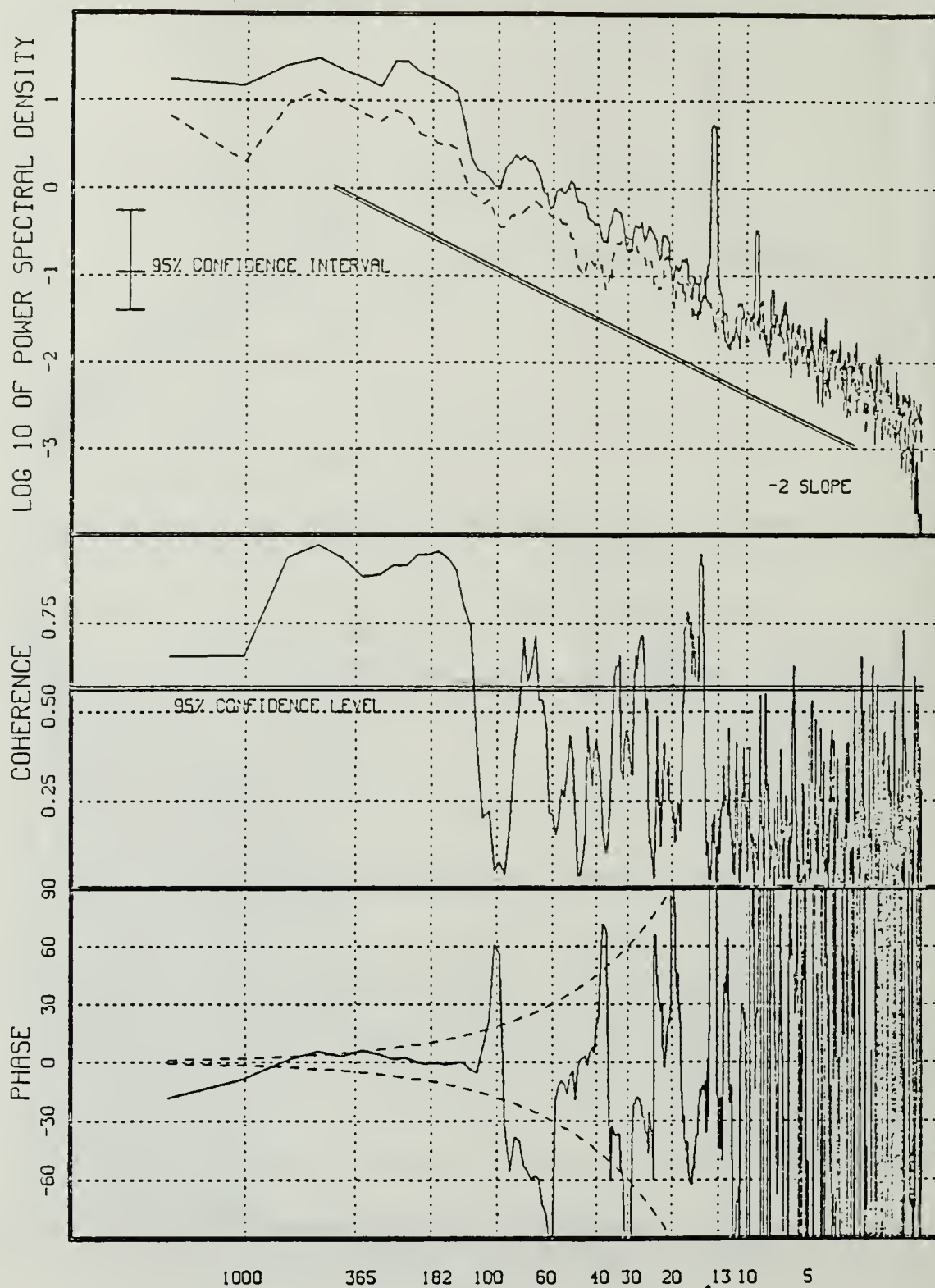


Fig. 14. Energy Density, Coherence, and Phase Spectra of  $\delta LOD_{USNO}$  and  $\delta LOD_{atm75}$ : As in Fig. 12 except the atmospheric signal is computed above  $15^\circ N$  and below  $15^\circ S$ .

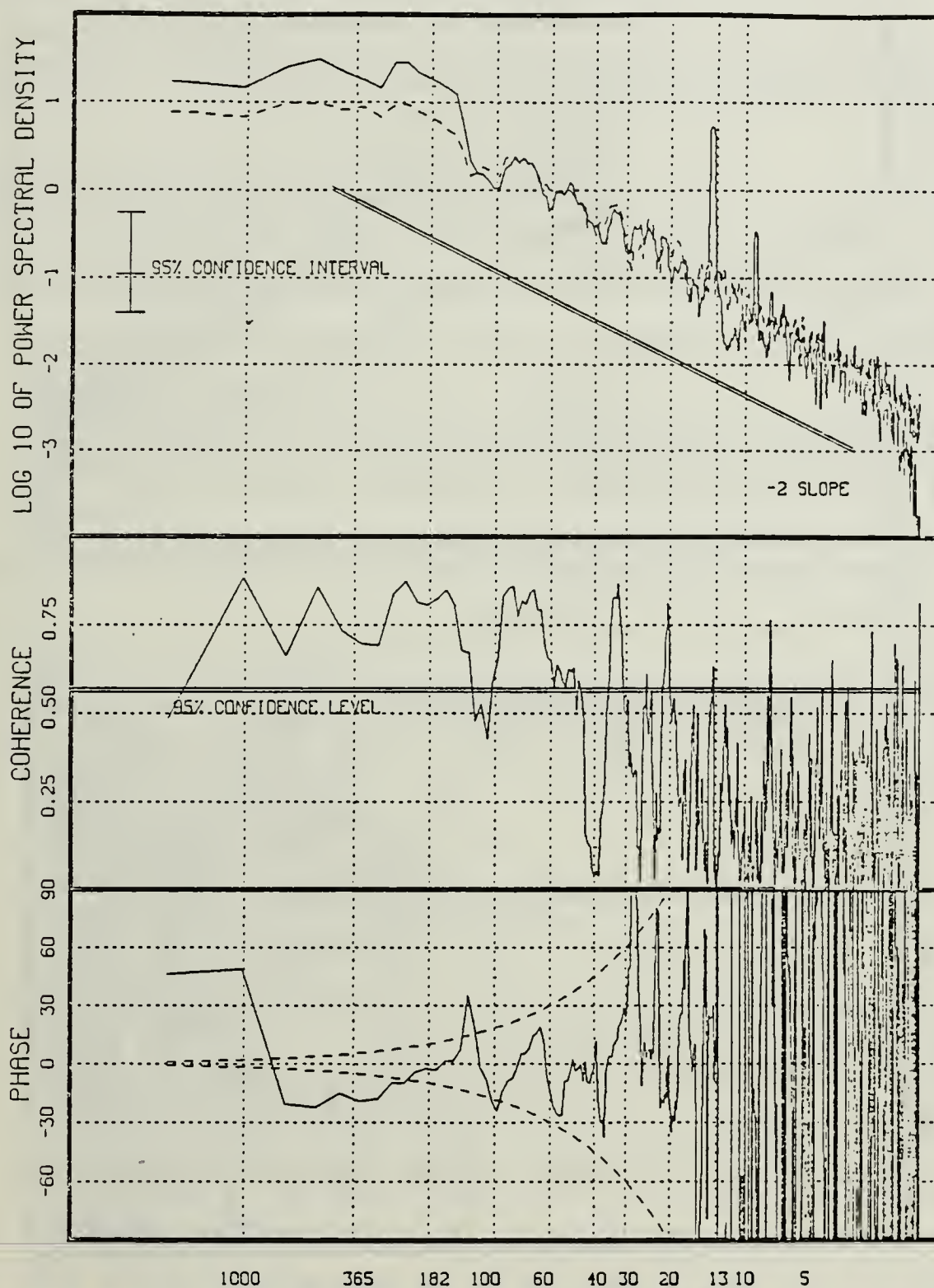


Fig. 15. Energy Density, Coherence, and Phase Spectra of  $\delta LOD_{USNO}$  and  $\delta LOD_{atm20}$ : As in Fig. 12 except the atmospheric signal is computed within  $20^\circ$  of the equator.

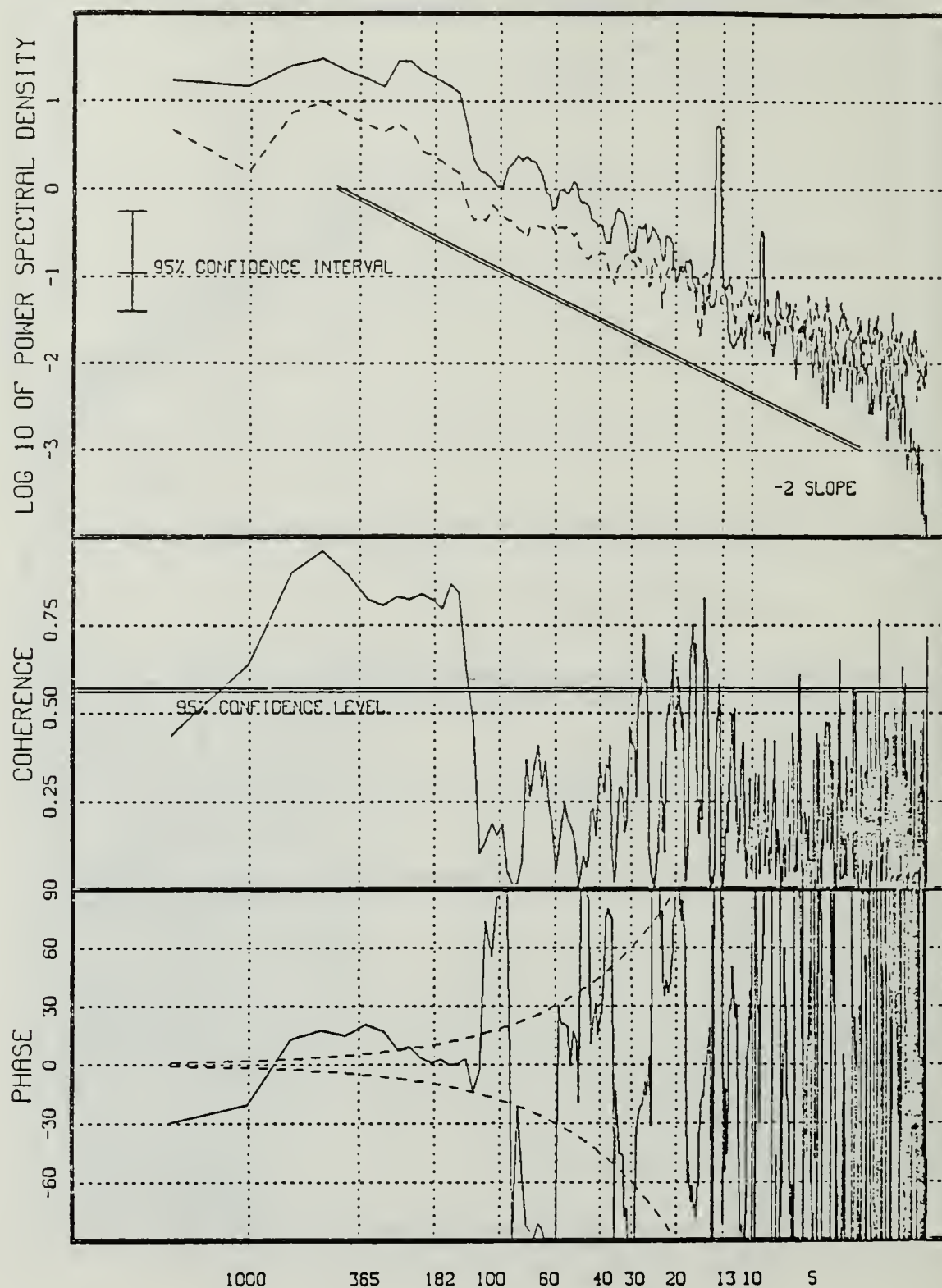


Fig. 16. Energy Density, Coherence, and Phase Spectra of  $\delta LOD_{USNO}$  and  $\delta LOD_{atm70^\circ}$ : As in Fig. 12 except the atmospheric signal is computed above  $20^\circ N$  and below  $20^\circ S$ .

[illegible]



```

DATA R /6370000.0/
C
  READ(05,INPUT)
  WRITE(06,INPUT)
C
  READ(05,1275) ((IDFELD(I,J),I=1,3),J=IDF1,IDF2)
1275 FORMAT(11(3A1,1X))
  WRITE(06,1276) ((IDFELD(I,J),I=1,3),J=IDF1,IDF2)
1276 FORMAT(1X,'FIELDS SELECTED ',11(3A1,1X))
C
  COUNT=0
  QQ=0
  NA=21135
  NB=0
  NCNT=0
  NFLE=0
C
C SET UP ARRAY FOR CALENDAR
  CALL KLNDR(CALNDR)
C SET UP COSINE ARRAY FOR INTEGRATION
  DO 2300 I=1, 37
    COSSQ(I) = (SIN(2.5*(I-1)*(2*PI/360.0))**2)
    COSSQ(74-I) = COSSQ(I)
2300 CONTINUE
C
  DO 10 I=1,6
  DO 10 J=1,8
  DO 10 K=1,6
10 KOUNT(I,J,K)=0
C
  IDHH1=IX1 - ((IX1/10000)*10000)
  IDD1=IDHH1/100
  IHH1=IDHH1 - IDD1*100
C
  CALL BUFFER(10,1,21135,IBUF)
C SKIP TO DESIRED DATA E.G. DEC 74 NSKPRC = 806
  CALL SKPREC(10,NSKPRC,&99,&999)
C
C IDFELD IS THE NEDN FIELD IDENTIFIER E.G. A01 = SLP
C F00=500 Z, T21 = 250MB V,
C
C IX1 & IX2 ARE THE DTG OF FIRST AND LAST PERIODS (FORM YYMMDDHH IN I8)
C
C ***** TOP OF DATA INPUT LOOP *****
  55 CONTINUE
C
C LONG RECORD FORMAT JUST USE ONE READ
  CALL GETREC(10,&99,&9999)
  NCNT=NCNT + 1
C
  CALL GBYTES(IBUF(1),IN1(1),00,06,00,24)
  CALL XBCD(24,IN1(1),BCD(1))
  CALL GBYTES(IBUF(6),IFTC,28,4,0,0)
  NFTC=IFTC*4
  CALL GBYTES(IBUF(16),KFTC(1),24,6,0,NFTC)
  CALL XBCD(NFTC,KFTC(1),FTC(1))

```



```

      CALL XINT(BCD,5,4,ITAU)
C
C ***** FORECAST HOUR ( TAU ) CHECK *****
      DO 610 K=1,NUMTAU
      NNTAU=K
      IF(ITAU.EQ. ITAUOK(K)) GOTO 620
610  CONTINUE
      GOTO 55
620  CONTINUE
C
C ***** CHECK YYMMDDHH TO GET THE DATA WE NEED *****
      CALL XINT(BCD,9,8,IYMDH)
      IF (IYMDH.LT. IX1) GO TO 55
      IF (IYMDH.GT. IX2) GO TO 77
      IDDHX=IYMDH - ((IYMDH/10000)*10000)
      IDDX=IDDHX/100
      IHX=IDDHX - IDDX*100
      NNDAY=(IDDX-IDD1) + (IABS(IHX-IH1)/12) + 1
C
C ***** DATA TYPE CHECK *****
C
      DO 640 K=IDF1,IDF2
      NNFLD=K
      DO 644 KK=1,3
644  IF(BCD(KK) .NE. IDFELD(KK,K)) GOTO 640
      GOTO 645
640  CONTINUE
      GOTO 55
645  CONTINUE
C
C *** DECODE SCALING INFORMATION, GRID SIZE
      CALL GBYTES(IBUF(6),IUNIT,8,5,0,0)
      CALL GBYTES(IBUF(6),ISCLE,13,6,0,0)
      CALL GBYTES(IBUF(6),KEYBIT,26,2,0,0)
      CALL GBYTES(IBUF(7),M,24,12,0,0)
      CALL GBYTES(IBUF(8),N,4,12,0,0)
      NR=M*N
C *** DECODE DATA ITSELF AFTER FINDING WHERE IT STARTS.
      NBITS = (21 + IFTC)*24
      IWDSRT = (NBITS/32) + 1
      ISKIP = NBITS - ((NBITS/32)*32)
      NBTSDP=16
      CALL GBYTES(IBUF(IWDSRT),IDATA,ISKIP,NBTSDP,0,NR)
C      CALL GBYTES(IBUF(27),IDATA,8,NBTSDP,0,NR)
C
C CDC HAS ONE'S COMPLEMENT, IBM HAS TWO'S COMPLEMENT FOR NEGATIVE'S.
      DO 30 I = 1,NR
30  IF (IDATA(I) .LT. 0) IDATA(I) = IDATA(I) + 1
C
C SET UP TO UNPACK 16 BIT DATA POINTS. THUS JDATA WHICH IS *2 HAS ONE
C DATA POINT PER WORD. DATA IS IN THE RIGHTMOST 16 BITS OF IDATA WHICH
C IS *4.
C
      L=0
      NR2=NR*2
      IF (ISCLE .LT. 32) GO TO 40

```

```

        ISL= 2** (ISCLE-32)
        DO 17 I = 2, NR2, 2
            L=L+1
            IDUM=JDATA(I)
17      DATA(L) = FLOAT(IDUM)/FLOAT(ISL)
        GO TO 45
    40    ISL=2** (32-ISCLE)
        DO 18 I=2, NR2, 2
            L=L+1
            IDUM=JDATA(I)
18      DATA(L)=FLOAT(IDUM)*FLOAT(ISL)
45      CONTINUE
C
C DBASE = 5574.0 FCTR = 0.01 FOR 500MB F00
C DBASE = 762.0 FCTR = 0.01 FOR 925MB R00
C DBASE = 0000.0 FCTR = 1.00 FOR SLP A01
C DBASE = 0000.0 FCTR =+0.01 FOR V AND 0.01 FOR U.
        DO 88 KZ=1, NR
    88    DATA(KZ)= DATA(KZ)*FCTR(NNFLD) + DBASE(NNFLD)
C
C ORIENT I,J INDICES SUCH THAT I=E-W      J=N-S
C REVERSE SENSE OF J SO THAT IT INCREASES NWD.
        DO 25 I=1, 73
            II=73 - (I-1)
            DO 25 J=1, 144
25      C(J,II)=D(I,J)
C
        IHR=IYMDH-(IYMDH/100)*100
        IDAY=((IYMDH-(IYMDH/10000)*10000)-IHR)/100
C *****ZONAL AVERAGING LOOP*****
C
2999 DO 2115 J = 1, 73
        AVG = 0.0
            DO 2116 I = 1, 144
                AVG = C(I,J) + AVG
2116      CONTINUE
        ZONAVG(NNFLD,J) = AVG/144.
2115 CONTINUE
C *****
        IF (NNFLD .EQ. 11) GOTO 3000
        GOTO 55
3000 QQ = QQ +1
        IF (IYMDH .NE. CALNDR(QQ)) GOTO 3500
        GOTO 3600
3500 WRITE(6,3501) QQ, CALNDR(QQ), LODATM(QQ)
3501 FORMAT(1X,I3,1X,I8,1X,F9.6,2X,'DATA MISSING FROM FNOC TAPES')
        GOTO 3000
C *****VERTICALLY INTEGRATE*****
3600 DO 2130 I=1, 73
        VERT(I) = (ZONAVG(1,I)+ZONAVG(2,I))*FACTRV(1)
&              + (ZONAVG(2,I)+ZONAVG(3,I))*FACTRV(2)
&              + (ZONAVG(3,I)+ZONAVG(4,I))*FACTRV(3)
&              + (ZONAVG(4,I)+ZONAVG(5,I))*FACTRV(4)
&              + (ZONAVG(5,I)+ZONAVG(6,I))*FACTRV(5)
&              + (ZONAVG(6,I)+ZONAVG(7,I))*FACTRV(6)
&              + (ZONAVG(7,I)+ZONAVG(8,I))*FACTRV(7)

```

```

      &          + (ZONAVG(8,I)+ZONAVG(9,I))*FACTRV(8)
      &          + (ZONAVG(7,I)+ZONAVG(8,I))*FACTRV(9)
2130 CONTINUE
C
C   APPLY COS LAT TERMS
      DO 2140 I=1, 73
2140 VERT(I) = VERT(I)*COSSQ(I)
C
C   HORIZONTALLY INTEGRATE
      AVERGE=0.0
      DO 2145 I=2,72
          AVERGE = VERT(I) + AVERGE
2145 CONTINUE
      AVERGE = AVERGE* PI/72.0
C
C   CONSTANTS OUTSIDE THE INTEGRAL ARE NOW BROUGHT IN:
      AVERGE = AVERGE*(2*PI*(R**3))/G
C   CALCULATE THE CHANGE IN LOD
      LODATM(QQ) = 1000.*(AVERGE*LODSID/(OMEGA*ISHELL))
C
      WRITE(6,3001) QQ, IYMDH, LODATM(QQ)
3001 FORMAT(1X,I3,1X,I8,1X,F9.6)
      GOTO 55
C
      99 CONTINUE
C
      77 WRITE(6,151) IYMDH
C   ***** OUTPUT LOOP *****
C
      WRITE (6,1020)
C      WRITE (6,1010) (LODATM(Q),Q=1,QQ)
1010 FORMAT(7F10.6)
1020 FORMAT(1X,'THESE ARE THE FINAL LOD VALUES IN SECONDS')
151 FORMAT(1X,'PGM ENDED OK IYMDH = ',I10)
C
C      DO 835 I=1,NNDAY
C      WRITE(06,1235) I,IX1
1235 FORMAT(1X,/,1X,'NDAY = ',I3,2X,'IX1 = ',I8)
835 CONTINUE
C
      CALL FILEND(IDF1,IDF2)
      STOP
C
C   ***** PARITY ERROR TRAP *****
9999 WRITE(06,120)
120 FORMAT(1X,' PARITY ERROR GETREC ')
      STOP
C   ***** SKPREC FAILURE *****
999 WRITE(06,122)
122 FORMAT(1X,' SKPREC FAILURE ')
      STOP
998 CONTINUE
      WRITE(06,1298) NFLE
1298 FORMAT(1X,' PGM ENDED.  NUMBER OF FILES PROCESSED = ',I4)
C      CALL FILEND(IDF1,IDF2)
      STOP

```

[illegible]



```

100 CONTINUE
    RETURN
    END
C ***** SUBROUTINE KLNDR *****
    SUBROUTINE KLNDR(CALNDR)
    INTEGER CALNDR(740),0
C   JAN (31 DAYS)
    CALNDR(1) = 87010100
    DO 5001 I=2,62,2
        CALNDR(I)=CALNDR(I-1) + 12
        CALNDR(I+1)=CALNDR(I-1) + 100
5001 CONTINUE
C   FEB (28 DAYS)
    CALNDR(63) = 87020100
    DO 5002 I=64,118,2
        CALNDR(I)=CALNDR(I-1) + 12
        CALNDR(I+1)=CALNDR(I-1) + 100
5002 CONTINUE
C   MAR (31 DAYS)
    CALNDR(119) = 87030100
    DO 5003 I=120,180,2
        CALNDR(I)=CALNDR(I-1) + 12
        CALNDR(I+1)=CALNDR(I-1) + 100
5003 CONTINUE
C   APR (30 DAYS)
    CALNDR(181) = 87040100
    DO 5004 I=182,240,2
        CALNDR(I)=CALNDR(I-1) + 12
        CALNDR(I+1)=CALNDR(I-1) + 100
5004 CONTINUE
C   MAY (31 DAYS)
    CALNDR(241) = 87050100
    DO 5005 I=242,302,2
        CALNDR(I)=CALNDR(I-1) + 12
        CALNDR(I+1)=CALNDR(I-1) + 100
5005 CONTINUE
C   JUN (30 DAYS)
    CALNDR(303) = 87060100
    DO 5006 I=304,362,2
        CALNDR(I)=CALNDR(I-1) + 12
        CALNDR(I+1)=CALNDR(I-1) + 100
5006 CONTINUE
C   JUL (31 DAYS)
    CALNDR(363) = 87070100
    DO 5007 I=364,424,2
        CALNDR(I)=CALNDR(I-1) + 12
        CALNDR(I+1)=CALNDR(I-1) + 100
5007 CONTINUE
C   AUG (31 DAYS)
    CALNDR(425) = 87080100
    DO 5008 I=426,486,2
        CALNDR(I)=CALNDR(I-1) + 12
        CALNDR(I+1)=CALNDR(I-1) + 100
5008 CONTINUE
C   SEP (30 DAYS)
    CALNDR(487) = 87090100

```

```

DO 5009 I=488,546,2
    CALNDR(I)=CALNDR(I-1) + 12
    CALNDR(I+1)=CALNDR(I-1) + 100
5009 CONTINUE
C OCT (31 DAYS)
    CALNDR(547) = 87100100
DO 5010 I=548,608,2
    CALNDR(I)=CALNDR(I-1) + 12
    CALNDR(I+1)=CALNDR(I-1) + 100
5010 CONTINUE
C NOV (30 DAYS)
    CALNDR(609) = 87110100
DO 5011 I=610,668,2
    CALNDR(I)=CALNDR(I-1) + 12
    CALNDR(I+1)=CALNDR(I-1) + 100
5011 CONTINUE
C DEC (31 DAYS)
    CALNDR(669) = 87120100
DO 5012 I=670,730,2
    CALNDR(I)=CALNDR(I-1) + 12
    CALNDR(I+1)=CALNDR(I-1) + 100
5012 CONTINUE
    RETURN
    END
C***** SUBROUTINE FILEND *****
    SUBROUTINE FILEND(IDSRT,IDEND)
C    KK1=(IDSRT + 1)*10
C    KK2=(IDEND + 1)*10
C    DO 778 KK=KK1, KK2, 10
C    DO 778 K=2, 02
C    IFILE = KK + (K - 1)
C 778 ENDFILE IFILE
C    ENDFILE 21
C    ENDFILE 22
C    ENDFILE 24
C    ENDFILE 26
    RETURN
    END

/*
//LKED.SYSLIB DD
// DD
// DD
// DD
// DD
// DD UNIT=3350,VOL=SER=MVS003,DISP=SHR,DSN=C1012.TAPEUT,
// LABEL=(,,IN)
/* NOTE ONLY ODD NUMBERED TAPES HAVE THE 00Z DATA AND 120HR FCSTS.
//GO.FT10F001 DD UNIT=3400-5,VOL=SER=W16733,
// DISP=(OLD,PASS),LABEL=(1,NL,,IN),
// DCB=(RECFM=FB,BLKSIZE=21135,DEN=4)
//GO.SYSIN DD *
&INPUT NSKPRC=00, IX1=87070100, IX2=87123112, IDF1=01, IDF2=9&END
C20 D20 E20 F20 G20 H20 I20 J20 K20
/*
//*/

```

## APPENDIX B. FORTRAN CODE FOR SPECTRAL ANALYSIS

```

C*****
C
C    ENERGY DENSITY, CROSS SPECTRUM, PHASE, AND COHERENCE
C    INPUT FILES ARE UNITS 33, 34, and 35
C    OUTPUT FILES ARE UNITS 41 THROUGH 45
C
C*****
C
C    PROGRAM CRSPEC
C    PARAMETER(N=2048,M=11)
C
C    DECLARE ARRAYS.
C    REAL*4 DATA(N), GX(N), GXSUM(N/2 + 1),ATM1(1622),ATM2(1622)
C    REAL*4 DATAY(N), GY(N), GYSUM(N/2 + 1),LOD(1622),LIMPH1(N/2+1)
C    REAL*4 DAY,XSUM(N/2+1),YSUM(N/2+1)
C    REAL*4 CXY(N), QXY(N), PHASE(N), COHER(N), FREQ(N),LIMPH2(N/2+1)
C    INTEGER*4 IWK(N+1),FILENO
C    COMPLEX AX(N), AY(N), GXY(N), GXYSUM(N/2 + 1), XYSUM(N/2+1)
C
C    CHARACTER*60 TITLE1,TITLE2,TITLE3,TITLE4,TITLE5,TITLE6,TITLE7
C    DEFINE CONSTANTS.
C    M AND N ARE DEFINED IN PARAMETER SECTION; N IS NUMBER OF SAMPLES
C    M IS THE POWER OF TWO TO GET N
C    XN = FLOAT(N)
C    NF = N/2 + 1
C    (NF IS INDEX VALUE FOR NYQUIST FREQ.)
C    DT = 1
C    (DT IS TIME BETWEEN SAMPLED VALUES)
C    T = FLOAT(N)
C    (T IS TOTAL TIME FOR SAMPLE; HERE IT IS EQUAL TO THE SAMPLE)
C    DF = 1./T
C    (DF IS DELTA F, FUNDAMENTAL FREQ.)
C    NS = 1
C    (NS IS NO. OF SAMPLES TO ENSEMBLE AVERAGE)
C    PI = 3.141593
C    W CORR = .875
C    (WINDOW CORRECTION)
C
C    INITIALIZE SUMMING ARRAYS.  RETAIN INFORMATION UP TO THE
C    NYQUIST FREQ. ONLY.
C    DO 100 I = 1, NF
C    GXSUM(I) = 0.
C    GYSUM(I) = 0.
C    GXYSUM(I) = (0.,0.)
100 CONTINUE
C
C***** MAIN LOOP OF PROGRAM *****
C COMPUTE ENERGY DENSITY SPECTRA AND ENERGY DENSITY CROSS SPECTRUM
C FOR EACH SAMPLE AND ENSEMBLE AVERAGE.
C
C    FILENO=45

```

```

      DO 500 K = 1, NS
C
C   READ DATA.
C   THIS IS FOR 15N/S DATA
      DO 144 I= 1, 1622
C     READ (34,209) ATM1(I)

C   BELOW IS ONLY FOR 20N TO 20S DATA.
C     READ (33,209) ATM1(I)
C     ATM1(I)=16./72.*ATM1(I)
C     READ (35,200) LOD(I),ATM1(I)
C     ATM1(I)=ATM2(I)-ATM1(I)
144  CONTINUE
C
200  FORMAT (2(1X,F9.6))
202  FORMAT (24X,F8.5)
209  FORMAT(10X,F9.6)

C   TAPER BOTH ENDS OF THE DATA
C
      CALL TAPER(1622,LOD)
      CALL TAPER(1622,ATM1)
C   ADD ZEROS
      DO 152 I=1,N
        IF ((I.LE. 213) .OR. (I.GT. 1835)) THEN
          DATAX(I)=0.
          DATAY(I)=0.
        ELSE
          DATAX(I)=LOD(I-213)
          DATAY(I)=ATM1(I-213)
        ENDIF
152  CONTINUE
C
C   WRITE (37,101) (DATAY(I),I=1,N)
101  FORMAT(8F8.4)
C   TRANSFER THE DATA TO COMPLEX ARRAYS AX AND AY FOR FFT2C INPUT.
C   NOTE THAT IN USING THE 2ND FORMULA IN FFT2C DOCUMENTATION, YOU
C   MUST INITIALLY TAKE THE COMPLEX CONJUGATE OF THE DATA.  SINCE
C   THE IMAGINARY PART IS ZERO, THIS STEP IS NOT NECESSARY.
      DO 300 I = 1, N
        AX(I) = CMPLX (DATAX(I), 0.)
        AY(I) = CMPLX (DATAY(I), 0.)
300  CONTINUE
C
C   DO FFT.
      CALL FFT2C (AX, M, IWK)
      CALL FFT2C (AY, M, IWK)
C
C   MAKE ADJUSTMENT TO GET 2ND FORMULA.
      DO 325 I = 1, N
        AX(I) = CONJG (AX(I)) / XN
        AY(I) = CONJG (AY(I)) / XN
325  CONTINUE
C
C   COMPUTE THE ENERGY DENSITY SPECTRA GX(F) AND GY(F) AND THE
C   CROSS SPECTRUM GXY(F) FROM FFT2C OUTPUT AX AND AY.

```



```

DO 350 I = 1, N
  GX(I) = CABS(AX(I)**2)*(2./DF)
  GY(I) = CABS(AY(I)**2)*(2./DF)
  GXY(I) = AY(I)*CONJG(AX(I))*(2./DF)
350 CONTINUE
C
C   SINCE YOU MUST ENSEMBLE AVERAGE THE RESULTS OVER THE NO. OF SAMPLES,
C   ADD GX(F), GY(F), GXY(F) INTO SUMMING ARRAYS.  NOTE THAT EACH
C   FREQUENCY IS SUMMED INDEPENDENTLY.
  DO 400 I = 1, NF
    GXSUM(I) = GXSUM(I) + GX(I)
    GYSUM(I) = GYSUM(I) + GY(I)
    GXYSUM(I) = GXYSUM(I) + GXY(I)
400 CONTINUE
C
  500 CONTINUE
C***** END OF MAIN LOOP *****
C
C   AFTER SUMMING IN ALL OF THE ESTIMATES, DIVIDE BY THE NO. OF
C   SAMPLES NS AND BY THE WINDOW CORRECTION FACTOR W CORR.
C   COMPUTE THE CO-SPECTRUM CXY, THE QUAD-SPECTRUM QXY, THE
C   PHASE SPECTRUM, AND THE COHERENCE SPECTRUM.  CONVERT THE
C   PHASE SPECTRUM TO DEGREES FOR PLOTTING.
  XNS = FLOAT(NS)
C   MULTIPLY BY F**2

  DO 600 I = 2, NF
    GXSUM(I) = (GXSUM(I) / (XNS * W CORR))*((FLOAT(I-1)*DF)**2)
    GYSUM(I) = (GYSUM(I) / (XNS * W CORR))*((FLOAT(I-1)*DF)**2)
    GXYSUM(I) = (GXYSUM(I) / (XNS * W CORR))*((FLOAT(I-1)*DF)**2)
600 CONTINUE

C   APPLY A 5 POINT SMOOTHING CURVE)

  DO 610 I=3,NF-2
    XSUM(I)=(GXSUM(I-1)+GXSUM(I)+GXSUM(I+1)+GXSUM(I-2)+GXSUM(I+2))/5.
    YSUM(I)=(GYSUM(I-1)+GYSUM(I)+GYSUM(I+1)+GYSUM(I-2)+GYSUM(I+2))/5.
    XYSUM(I)=(GXYSUM(I-1)+GXYSUM(I)+GXYSUM(I+1)+GXYSUM(I-2)
    &          +GXYSUM(I+2))/5.
610 CONTINUE
    XSUM(2)=(GXSUM(2)+GXSUM(3))/2.
    YSUM(2)=(GYSUM(2)+GYSUM(3))/2.
    XYSUM(2)=(GXYSUM(2)+GXYSUM(3))/2.

    XSUM(3)=(GXSUM(2)+GXSUM(3)+GXSUM(4))/3.
    YSUM(3)=(GYSUM(2)+GYSUM(3)+GYSUM(4))/3.
    XYSUM(3)=(GXYSUM(2)+GXYSUM(3)+GXYSUM(4))/3.

C   RETURN VALUES TO ARRAYS
  DO 676 I=1,NF
    GXSUM(I)=XSUM(I)
    GYSUM(I)=YSUM(I)
    GXYSUM(I)=XYSUM(I)
676 CONTINUE
C

```

```

C   CREATE FREQUENCY ARRAY AS MULTIPLES OF THE FUNDAMENTAL FREQ. DF.
C   NOTE THAT THE FIRST BIN IS THE MEAN AND THE FREQ. IS ZERO.
      DO 700 I = 1, NF
        FREQ(I) = FLOAT(I-1) * DF
700  CONTINUE
      DO 615 I=2,NF
        CXY(I) = REAL(GXYSUM(I))
        QXY(I) = AIMAG(GXYSUM(I))
        IF (CXY(I) .EQ. 0.) THEN
          PHASE(I) = 0.
          GOTO 679
        ENDIF
        PHASE(I) = ATAN2(QXY(I),CXY(I))*(180./PI)
        IF (PHASE(I) .GE. 90.) PHASE(I)=90.
        IF (PHASE(I) .LE. -90.) PHASE(I)=-90.
679  IF ((GXSUM(I)*GYSUM(I)) .EQ. 0.) THEN
        COHER(I)=0.
        GOTO 615
      ENDIF
      COHER(I) = ((CXY(I)**2)+(QXY(I)**2))/(GXSUM(I)*GYSUM(I))
615  CONTINUE
C   DIVIDE BY F**2
      DO 611 I=2,NF
        GXSUM(I)=GXSUM(I)/((FLOAT(I-1)*DF)**2)
        GYSUM(I)=GYSUM(I)/((FLOAT(I-1)*DF)**2)
        GXYSUM(I)=GXYSUM(I)/((FLOAT(I-1)*DF)**2)
611  CONTINUE
C
C   SET LIMITS FOR PHASE PLOT
      DAY=5.0
      DO 833 I=2,NF
        LIMPH1(I)=FREQ(I)*DAY*360
        IF (LIMPH1(I).GE. 90.) LIMPH1(I)=90.
        LIMPH2(I)= -LIMPH1(I)
833  CONTINUE
C   PRINT OUT FREQ. , GXSUM(F), GYSUM(F), CXY(F), QXY(F), PHASE(F),
C   COHER(F).
1005 FORMAT(14X,'X',9X,'Y',9X,'CO-',6X,'QUAD')
1010 FORMAT(1X,'FREQUENCY',2X,'SPECTRUM',3X,'SPECTRUM',2X,'SPECTRUM',
      &2X,'SPECTRUM',4X,'PHASE',2X,'COHERENCE')
1015 FORMAT(1X,72(' '))
C   WRITE(36,1005)
C   WRITE(36,1010)
C   WRITE(36,1015)
      DO 800 I = 2, 4
        WRITE(FILENO,810)FREQ(I),GXSUM(I),GYSUM(I),PHASE(I),
      & COHER(I),LIMPH1(I),LIMPH2(I)
800  CONTINUE
      DO 802 I = 5, NF-5, 5
        DO 844 K=1,5
          WRITE(FILENO,810)FREQ(K+I),GXSUM(I+3),GYSUM(I+3),PHASE(I+3),
      & COHER(I+3),LIMPH1(K+I),LIMPH2(K+I)
844  CONTINUE
802  CONTINUE
810  FORMAT(7F10.5)

```

```

C   COMPUTE THE VARIANCE BY INTEGRATING GXSUM(F) AND GYSUM(F)
C   NUMERICALLY BY SUMMING GXSUM(F)*DF AND GYSUM(F)*DF OVER THE
C   APPROPRIATE RANGE OF FREQUENCIES.  WRITE OUT THE VARIANCES.
      SUM = 0.
      SUMM = 0.
      DO 900 I = 1, NF
        PRODX = GXSUM(I)*DF
        PRODY = GYSUM(I)*DF
        SUM = SUM + PRODX
        SUMM = SUMM + PRODY
900  CONTINUE
      WRITE(FILENO,910) SUM
      WRITE(FILENO,920) SUMM
910  FORMAT(//,4X,'VARIANCE OF LOD SERIES = ',F9.3)
920  FORMAT(//,4X,'VARIANCE OF ATM SERIES = ',F9.3)

C   COMPUTE THE CO-VARIANCE BY INTEGRATING THE CO-SPECTRUM CXY(F).
C   WRITE OUT THE CO-VARIANCE.
      S = 0.
      DO 2000 I = 1, NF
        PRODXY = CXY(I)*DF
        S = S+ PRODXY
2000 CONTINUE
      WRITE(FILENO,2010) S
2010 FORMAT(//,4X,'COVARIANCE = ',F9.3)
      STOP
      END

      SUBROUTINE TAPER(NTS,X)
C   MULTIPLYING INPUT DATA BY TAPER FUNCTION
      DIMENSION X(NTS)
      PI = 3.1415927
      XNTS = NTS
      MA = 0.1*XNTS
      MB = XNTS-MA
      DO 204 I = 1,NTS
        IF(I.LE.MA) GO TO 201
        IF(I.GE.MB) GO TO 202
        GO TO 204
202  XI=NTS-I
        GO TO 203
201  XI=I-1
203  ARG = 5.0*PI*XI/XNTS
        X(I) = X(I)*(1.-COS(ARG)*COS(ARG))
204  CONTINUE
      RETURN
      END

      SUBROUTINE MINMAX (A,N,AMIN,AMAX)
C
      DIMENSION A(1)
C
      AMIN = A(1)
      AMAX = A(1)
C
      DO 100 I = 1, N

```

```
        IF (A(I) .LT. AMIN) AMIN = A(I)
        IF (A(I) .GT. AMAX) AMAX = A(I)
100    CONTINUE
C
    RETURN
END
```



## APPENDIX C. FREQUENCY RESPONSE OF DIGITAL FILTERS

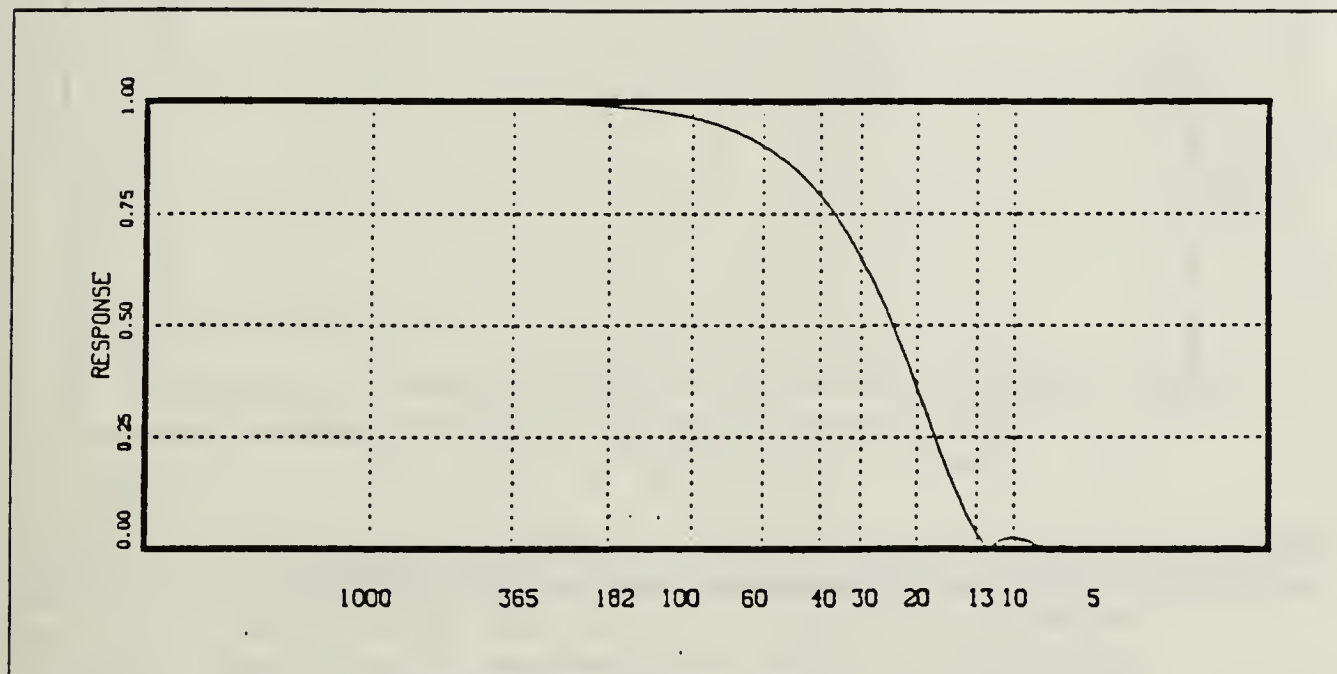


Fig. 17. Spectral response of 23-point  $\sin^2$  weighted filter: Lowpass filter designed primarily to remove solid body tides at 7 and 13.5 days from  $\delta LOD_{USNO}$  data.

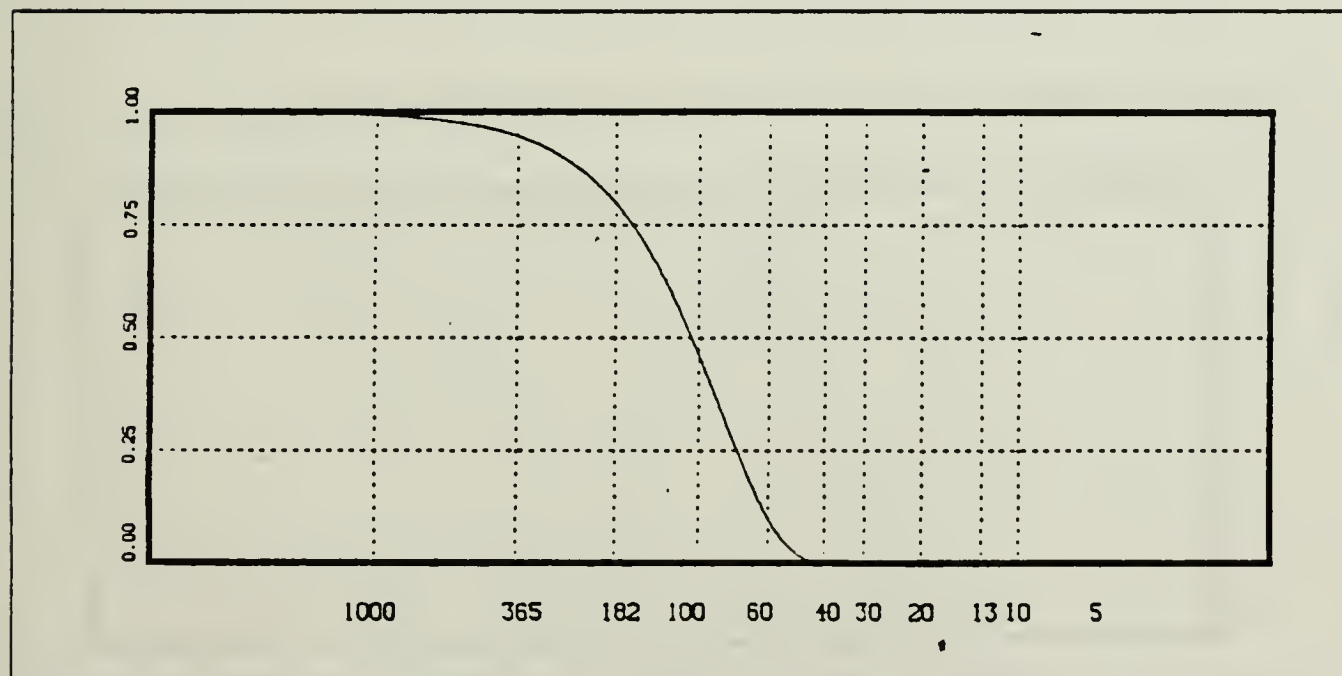


Fig. 18. Spectral response of a twice run 75-point  $\sin^2$  filter: Lowpass design permitted removal of most subseasonal components. Note the absence of side lobes, as well as the relative steepness achieved by running the filter twice.

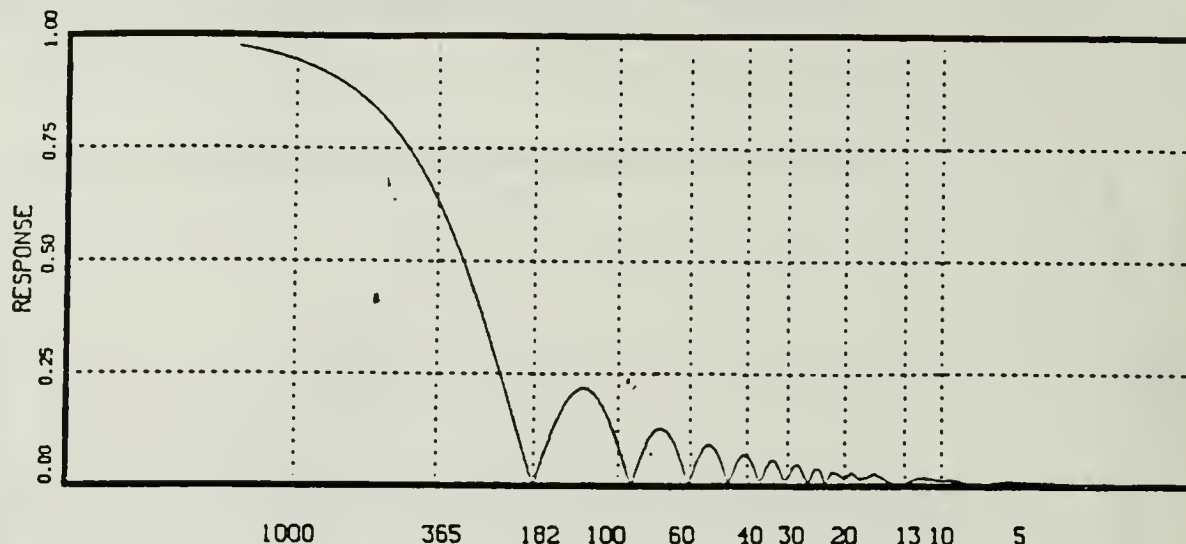


Fig. 19. Response of 183-point unweighted moving average filter: Used to isolate annual terms. A weighted filter would have required too many-points, and would not have sufficient vertical steepness to include annual frequencies. Still, almost 35% of the annual signal is attenuated in order to filter out the semiannual terms.

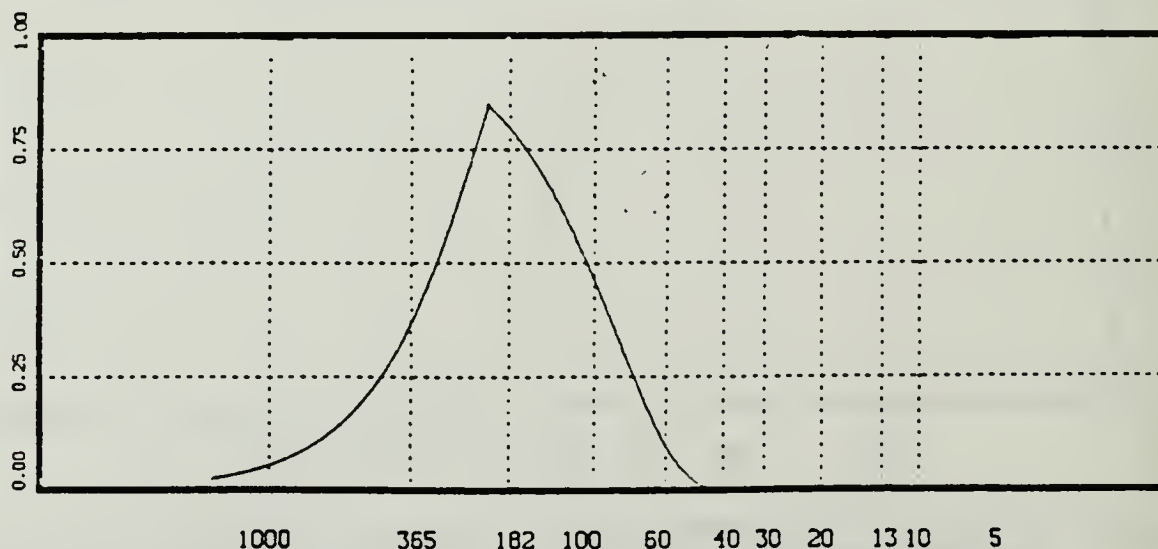


Fig. 20. Filter to isolate semiannual terms: Combination of twice run 75-point  $\sin^2$  weighted filter and 183-point unweighted subtraction moving average. Maximum response is at about 200 days.

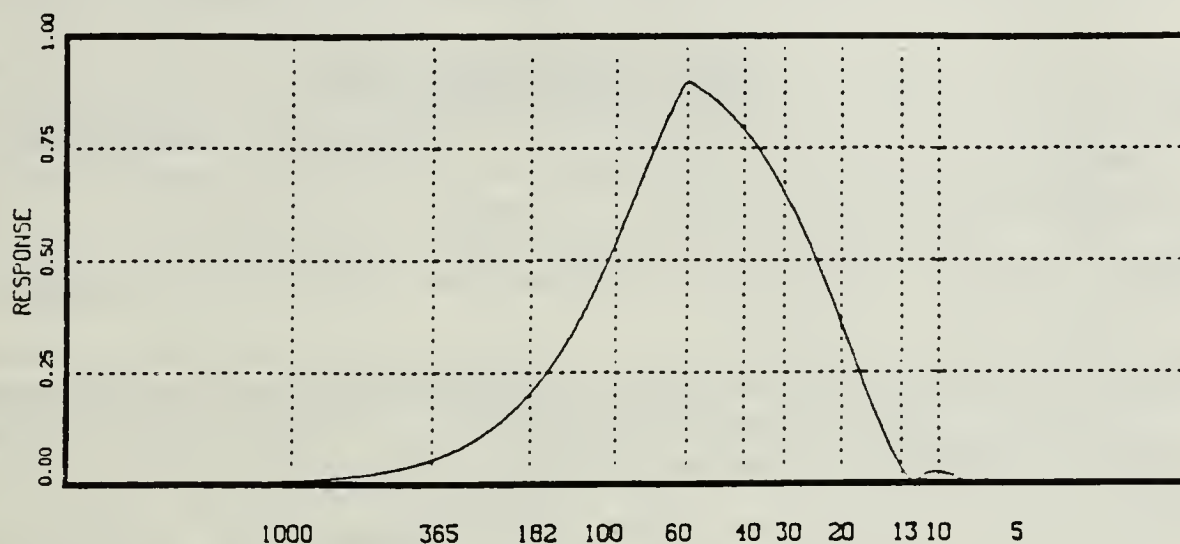


Fig. 21. Subseasonal isolation filter: Combination of twice run 75-point weighted moving average (see Fig. 19) and 23-point weighted moving average. Peak response is at 60 days.

## LIST OF REFERENCES

- Barnes, R.T.H., R. Hide, A.A. White, and C.A. Wilson, 1983: Atmospheric angular momentum fluctuations, length-of-day changes and polar motion. *Proc. R. Soc. London, Ser. A* **387**, 31-73.
- Bendat, J.S., and A.G. Piersol, 1971: Random Data: Analysis and Measurement Procedures. John Wiley & Sons.
- Dickey, J.O., T.M. Eubanks, and J. A. Steppe, 1986: High accuracy earth rotation and atmospheric angular momentum. *Earth Rotation: Unsolved Problems*, A. Cazenave, editor. D. Riedel Publishing Co. 137-162.
- Eubanks, T.M., J.A. Steppe, J.O. Dickey, and P.S. Callahan, 1985: A spectral analysis of the earth's angular momentum budget. *J. Geophys. Res.*, **90**, 5385-5404.
- Eubanks, T.M., J.A. Steppe and J.O. Dickey, 1986: The El Nino, the southern oscillation and the earth rotation. *Earth Rotation: Unsolved Problems*, A. Cazenave, editor. D. Riedel Publishing Co. 163-186.
- Jenkins, G.M. and D.G. Watts, 1968: Spectral Analysis and its applications. Holden-Day, San Francisco.
- Lambeck, K. and A. Cazenave, 1974: The earth's variable rotation and atmospheric circulation. II, the continuum. *Geophys J.* **38**, 49-61.
- Lambeck, K., 1980: The Earth's Variable Rotation. Cambridge University Press, New York.
- Langley, R.B., R.W. King, I.I. Shapiro, R.D. Rosen, and D.A. Salstein, 1981: Atmospheric angular momentum and the length of the day: A common fluctuation with a period near 50 days. *Nature*, **294**, 730-733.
- Madden, R.A. and P.R. Julian, 1971: Detection of a 40-50 day oscillation in the zonal wind in the tropical pacific. *J. Atmos. Sci.* **28** 702-708.
- Madden, R.A. and P.R. Julian, 1972: Description of Global-scale circulation cells in the tropics with a 40-50 day period. *J. Atmos. Sci.*, **29**, 1109-1123.
- Morgan, P.J., R.W. King, and I.I. Shapiro, 1985: Length of day and atmospheric angular momentum: A comparison for 1981-1983. *J. Geophys. Res.*, **90** 12645-12652.
- Munk, W.H., and G.I.F. MacDonald, 1960: The Rotation of the Earth. Cambridge University Press, New York.
- Ramsey, N.F., 1988: Precise measurement of time. *American Scientist* , **76**, 42-49.
- Robinson, E.A. and M.T. Silvia, 1978: Digital Signal Processing and Time Series Analysis. Holden-Day, San Francisco.



- Rosen, R.D., and D.A. Salstein, 1983: Variations in atmospheric angular momentum on global and regional scales and the length of day. *J. Geophys. Res.*, **88**, 5451-5470.
- Rosen, R.D., and D.A. Salstein, 1985: Contributions of stratospheric winds to annual and semiannual fluctuations in atmospheric angular momentum and length of day. *J. Geophys. Res.*, **90**, 8033-8041.
- Rosen, R.D., D.A. Salstein, T.M. Eubanks, J.O. Dickey, and J.A. Steppe, 1984: An El Nino signal in atmospheric angular momentum and earth rotation. *Science*, **225**, 411-414.
- Swinbank, R., 1985: The global atmospheric angular momentum balance inferred from analyses made during the FGGE. *Quart. J. Roy. Meteor. Soc.*, **111**, 977-992.
- Wolf, W.L. and R.B. Smith, 1987: Length-of-day changes and mountain torque during El Nino. *J. Atmos. Sci.*, **44**, 3656-3660

## INITIAL DISTRIBUTION LIST

	No. Copies
1. Defense Technical Information Center Cameron Station Alexandria, VA 22304-6145	2
2. Library, Code 0142 Naval Postgraduate School Monterey, CA 93943-5002	2
3. Chief of Naval Research 800 N. Quincy Street Arlington, VA 22217-5000	1
4. Director Naval Oceanography Division Naval Observatory 34th and Massachusetts Avenue NW Washington, DC 20390-5000	1
5. Denis McCarthy Chief Earth Orientation, Parameters Division Naval Observatory 34th and Massachusetts Avenue NW Washington, DC 20390-5100	1
6. Commander Naval Oceanography Command NSTL, MS 39522-5000	1
7. Commanding Officer Fleet Numerical Oceanography Center Monterey, CA 93943-5000	1
8. Commanding Officer Naval Oceanographic Office NSTL, MS 39522-5000	1
9. Chairman (Code 63Rd) Department of Meteorology Naval Postgraduate School Monterey, CA 93943-5000	1
10. Chairman (Code 68Co) Department of Oceanography Naval Postgraduate School Monterey, CA 93943-5000	1

11. Professor Robert L. Haney (63Hy) 2  
Naval Postgraduate School  
Monterey, CA 93943-5000
  
12. Professor William J. Shaw (63Sh) 1  
Naval Postgraduate School  
Monterey, CA 93943-5000
  
13. CDR William L. Benedict 4  
4376 Mt. Helix Highlands Dr.  
La Mesa, CA 92041
  
14. Commanding Officer 1  
Naval Ocean Research and Development Activity  
NSTL  
Bay St Louis, MS 39522-5000
  
15. Commanding Officer 1  
Naval Environmental Prediction  
Research Facility  
Monterey, CA 93943-5000
  
16. Chairman, Oceanography Department 1  
U.S. Naval Academy  
Annapolis, MD 21402-5000
  
17. Office of Naval Research (Code 420) 1  
Naval Ocean Research and Development  
Activity  
800 N. Quincy Street  
Arlington, VA 22217-5000
  
18. Commander 1  
Oceanographic Systems Pacific  
Box 1390  
Pearl Harbor, HI 96860-5000
  
19. Commander (AIR-370) 1  
Naval Air Systems Command  
Washington, DC 20360-5000
  
20. Library Acquisitions 1  
National Center for Atmospheric Research  
P.O. Box 3000  
Boulder, CO 80307-5000
  
21. Roland Madden 1  
National Center for Atmospheric Research  
P.O. Box 3000  
Boulder, CO 80307-5000

22. Jean O. Dickey  
Jet Propulsion Laboratory  
California Institute of Technology  
4800 Oak Grove Drive  
Pasadena, CA 91109

















Thesis  
B36646 Benedict  
c.1 Atmospheric angular  
momentum and length of  
day.

Thesis  
B36646 Benedict  
c.1 Atmospheric angular  
momentum and length of  
day.



Atmospheric angular momentum and length



3 2768 000 78063 9  
DUDLEY KNOX LIBRARY